2003

Analysis of measurements of Saharan dust by airborne and ground-based remote sensing methods during the Puerto Rico Dust Experiment (PRIDE)

Analysis of measurements of Saharan dust by airborne and ground-based remote sensing methods during the Puerto Rico Dust Experiment (PRIDE)

Jeffrey S. Reid,[1,2] James E. Kinney,[1] Douglas L. Westphal,[2] Brent N. Holben,[3] Ellsworth J. Welton,[3] Si-Chee Tsay,[3] Daniel P. Eleuterio,[4] James R. Campbell,[5] Sundar A. Christopher,[7] P. R. Colarco,[8] Haflidi H. Jonsson,[4] John M. Livingston,[9] Hal B. Maring,[10] Michael L. Meier,[11] Peter Pilewskie,[12] Joseph M. Prospero,[10] Elizabeth A. Reid,[2] Lorraine A. Remer,[3] Philip B. Russell,[12] Dennis L. Savoie,[10] Alexander Smirnov,[6] and Didier Tanré[13]

Received 29 April 2002; revised 10 October 2002; accepted 16 December 2002; published 7 August 2003.

[1] For 26 days in mid-June and July 2000, a research group comprised of U.S. Navy, NASA, and university scientists conducted the Puerto Rico Dust Experiment (PRIDE). In this paper we give a brief overview of mean meteorological conditions during the study. We focus on our findings on African dust transported into the Caribbean utilizing a Navajo aircraft and AERONET Sun photometer data. During the study midvisible aerosol optical thickness (AOT) in Puerto Rico averaged 0.25, with a maximum >0.5 and with clean marine periods of ~0.08. Dust AOTs near the coast of Africa (Cape Verde Islands and Dakar) averaged ~0.4, 30% less than previous years. By analyzing dust vertical profiles in addition to supplemental meteorology and MPLNET lidar data we found that dust transport cannot be easily categorized into any particular conceptual model. Toward the end of the study period, the vertical distribution of dust was similar to the commonly assumed Saharan Air Layer (SAL) transport. During the early periods of the study, dust had the highest concentrations in the marine and convective boundary layers with only a weak dust layer in the SAL being present, a state usually associated with wintertime transport patterns. We corroborate the findings of *Maring et al.* [2003] that in most cases, there was an unexpected lack of vertical stratification of dust particle size. We systematically analyze processes that may impact dust vertical distribution and speculate that dust vertical distribution predominately influenced by flow patterns over Africa and differential advection coupled with fair weather cloud entrainment, mixing by easterly waves, and regional subsidence. *INDEX TERMS:* 0305 Atmospheric Composition and Structure: Aerosols and particles (0345, 4801); 0330 Atmospheric Composition and Structure: Geochemical cycles; 0360 Atmospheric Composition and Structure: Transmission and scattering of radiation; 0368 Atmospheric Composition and Structure: Troposphere—constituent transport and chemistry; *KEYWORDS:* dust, aerosol, meteorology, Sahara, vertical distribution, Caribbean

Citation: Reid, J. S., et al., Analysis of measurements of Saharan dust by airborne and ground-based remote sensing methods during the Puerto Rico Dust Experiment (PRIDE), *J. Geophys. Res.*, *108*(D19), 8586, doi:10.1029/2002JD002493, 2003.

[1]Space and Naval Warfare Systems Center-San Diego, San Diego, California, USA.
[2]Naval Research Laboratory, Monterey, California, USA.
[3]NASA Goddard Space Flight Center, Greenbelt, Maryland, USA.
[4]Naval Postgraduate School, Monterey, California, USA.
[5]Science Systems and Applications, Inc., Greenbelt, Maryland, USA.
[6]University of Maryland Baltimore County, Baltimore, Maryland, USA.
[7]Department of Atmospheric Sciences, University of Alabama, Huntsville, Alabama, USA.
[8]Laboratory for Atmospheric and Space Physics, Program in Atmospheric and Oceanic Sciences, University of Colorado, Boulder, Colorado, USA.
[9]SRI International, Menlo Park, California, USA.
[10]Rosenstiel School of Marine and Atmospheric Science, University of Miami, Miami, Florida, USA.
[11]Material Science and Chemical Engineering, University of California, Davis, California, USA.
[12]NASA Ames Research Center, Mountain View, California, USA.
[13]Laboratoire d'Optique Atmospherique, CNRS Universite des Sciences et Technologies de Lille, Villeneuve d'Ascq, France.

0148-0227/03/2002JD002493$09.00

1. Introduction

[2] African dust outbreaks into the Mediterranean and north tropical Atlantic Ocean have been studied for decades [e.g., *Delany et al.*, 1967; *Prospero and Carlson*, 1972; *Ganor and Mamane*, 1982]. The Caribbean region, northern South America and the extreme North American southeast have been recognized as important receptor sites for dust transported in the trade winds [e.g., *Prospero et al.*, 1981; *Talbot et al.*, 1990; *Swap et al.*, 1992, 1996a, 1996b; *Westphal et al.*, 1987; *Perry et al.*, 1997; *Formenti et al.*, 2001]. Such transport has been found to be significant in the regions' geochemical cycles, radiative balance and air quality [e.g., *Duce et al.*, 1991; *Swap et al.*, 1992; *Tegen and Fung*, 1996; *Prospero*, 1999; *Gao et al.*, 2001]. Further, dust interferes with remote retrievals of such quantities as sea surface temperature [*May et al.*, 1992] and ocean color [*Moulin et al.*, 2001].

[3] Saharan dust transport mechanisms into the Caribbean region have been thought to be qualitatively understood for some time (e.g., early analysis by *Carlson and Prospero* [1972]). Subsequent modeling studies and some experimental evidence suggested that the predominant mode involves warm and dry dust-laden air (the Saharan Air Layer, or SAL) being advected off the African continent in the easterly trade winds. These easterly trade winds subsequently slide over the westerly near-surface onshore flow of the African monsoon [e.g., *Westphal et al.*, 1987; *Karyampudi and Carlson*, 1988]. The theory then suggested that dust is most prevalent in the free troposphere where it is rapidly transported across the Atlantic into the Caribbean region in 5 to 8 days.

[4] Despite this qualitative understanding, there is little quantitative data on dust aloft. Sporadic field studies and some lidar work have supported the idea that this is the dominant transport mechanism [e.g., *Prospero and Carlson*, 1972; *Karyampudi et al.*, 1999], but no long-term record exists of dust vertical distribution to test this hypothesis. In the last several years, it has been realized that a low-level transport mechanism can occur. *Chiapello et al.* [1995] recognized that during the winter months the near-surface onshore monsoonal flow required to give the "classical SAL" transport can weaken, allowing dust to be transported from Africa to sea at lower levels. *Formenti et al.* [2001] then reported dust in both elevated "SAL" and planetary boundary layers for several days in March 1998 when dust was transported into the Amazon Basin. Even in the middle of the dust season, *Karyampudi et al.* [1999] noted that "residual" dust can be found in the marine layer underneath the SAL. Recently, in a study describing the vertical distribution of dust found at Puerto Rico during PRIDE, *Reid et al.* [2002] speculated that dust can be transported to the Caribbean region at lower levels well into the Northern Hemisphere summer. These recent studies have made it clear that dust transport out of Africa is more complicated than may have been first assumed.

[5] Uncertainty in dust's vertical distribution causes large uncertainties in many scientific fields including climate, cloud physics, satellite meteorology, geochemical cycles and air quality. In particular, recent sensitivity studies on the effects of dust on the atmosphere's radiative balance have pointed to dust vertical distribution as an important factor for radiative forcing at long IR wavelengths [e.g., *Claquin et al.*, 1998; *Myhre and Stordal*, 2001]. Hence correct dust vertical distribution parameterizations are imperative to modelers attempting to analyze the impact of dust on surface, atmosphere, and top of atmosphere energetics [e.g., *Sokolik et al.*, 2001]. Even if free tropospheric SAL transport were the only mechanism of transport into the Caribbean region, correctly modeling dust transport across the trade inversion into the marine boundary layer would be a non-trivial task for transport modeling. However, given the true variability in dust vertical profiles, modeling and parameterizing dust transport is formidable. Clearly a two-dimensional satellite image of regional optical depth is difficult to interpret for the three-dimensional issues of ocean fertilization, particle concentration at cloud levels for indirect effect studies, and atmospheric visibility.

[6] The Puerto Rico Dust Experiment (PRIDE) was conducted in July 2000 to better understand the issues of dust transport and radiative forcing in the north subtropical Atlantic Ocean. Based out of Naval Station Roosevelt Roads on the eastern shore of Puerto Rico, PRIDE utilized a combination of aircraft, remote sensing and ground based assets to study African dust that is transported into the Caribbean region (Figure 1). In this study we begin with an overview of the mission assets with a description of the Navajo research aircraft, AERONET Sun photometers, and micropulse lidar used in the campaign. This is followed by a description of the general transport meteorology and dust coverage of the Caribbean during the study. Emphasis is placed on the third portion of this paper where we present in situ and ground based remote sensing measurements of dust vertical distribution and expand on the preliminary work of *Reid et al.* [2002]. This data gives a fairly complete picture as to dust characteristics and transport in the Caribbean during the PRIDE campaign. Results are then analyzed in the context of the fundamental processes that influence dust vertical distribution during transport. Finally, we discuss how our results fit with previous conceptual models.

2. Navajo Research Aircraft

[7] The principal aircraft used for PRIDE was a twin-engine, 8-seat Piper Navajo owned and operated by Gibbs Flite Center and contracted by SSC San Diego. During PRIDE, the Navajo flew 21 flights (61 hours of data collection over eighty flight hours) near the islands of Puerto Rico, St. Thomas, and St. Croix (Figure 1b).

[8] An overview of the Navajo is presented in Figure 2. The Navajo carried a Trimble GPS to provide latitude, longitude, altitude, and vector quantities. A supplemental Trimble TANSVector differential GPS navigational system provided a backup of these quantities as well as pitch (±0.3°), roll (±0.3°) and azimuth (+0.5°).

[9] State variable instrumentation included a pressure probe, two temperature probes, and two dew point/relative humidity probes. The static pressure probe was calibrated to ±0.4 mb accuracy. Through the entire study period, temperature values from the Navajo Rosemont and Vaisala probes and frequently released radiosondes from the surface were within ±0.3°C without correction. The EdgeTech dew

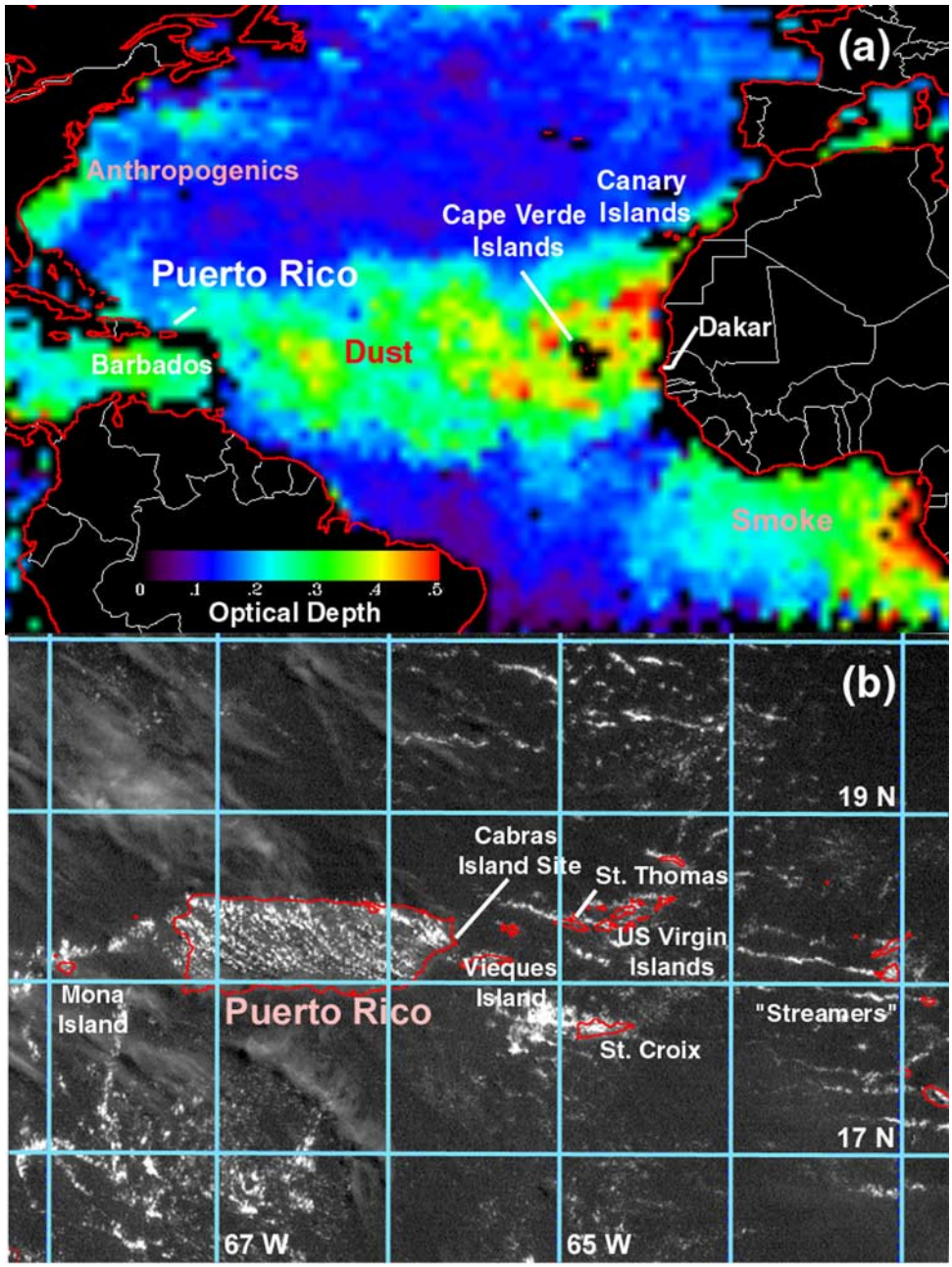

Figure 1. (a) Monthly averaged AVHRR Pathfinder aerosol optical thickness of the north subtropical Atlantic Basin for the month of July 2000. (b) GOES 8 visible image for the Caribbean region at 15:30 UTC on 5 July 2000.

point hygrometer (±0.5°C), Vaisala relative humidity probes (±5%) and radiosondes were within ±0.5°C of dew point.

[10] Radiation instruments onboard included a six-channel autotracking Sun photometer, upwelling and downwelling hyperspectral radiometers, a hyperspectral upwelling radiance instrument, and an Everest infrared thermometer for measuring sea surface temperature. Optical depth measurements were made by the six channel NASA Ames Airborne Sun photometer (AATS-6) at wavelengths of 380, 451, 526, 861 and 1021 nm [*Matsumoto et al.*, 1987]. A sixth channel at 970 nm was used to measure column integrated water vapor. Vertical profiles of AOT were then used to derive profiles of light extinction under cloud free conditions. A study of AATS-6 observations during PRIDE is given by *Livingston et al.* [2003].

[11] Upwelling and downwelling solar fluxes were measured with the NASA Ames Solar Spectral Flux Radiometer (SSFR). The SSFR is a moderate resolution flux (irradiance) spectrometer covering the wavelength range from 300 nm to 1700 nm with a resolution of 9 to 12 nm over the spectra range. Detailed findings from the SSFR data are given by P. Pilewskie et al. (Solar spectral radiative forcing by dust aerosol during PRIDE, manuscript in preparation, 2003). The spectral reflectance of the ocean's surface in the 350 to 2500 nm range was characterized with a FR-Pro spectrometer from Analytical Spectral Devices Inc. The resolution is

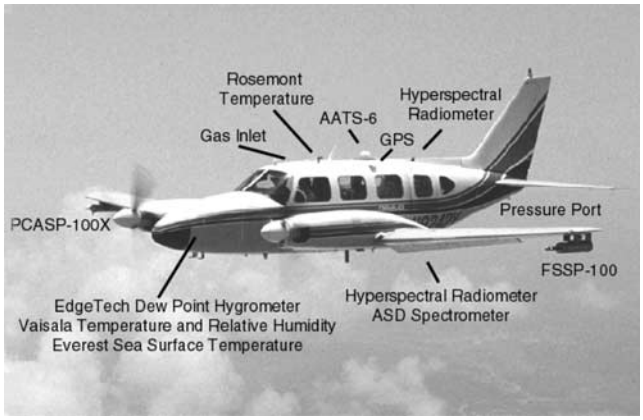

Figure 2. Picture of SSC San Diego Navajo taken during PRIDE and annotated with instrument placements (photo by Hal Maring, University of Miami).

3 nm in the range 350–1000 nm and 10 nm for longer wavelengths. An 18 degree field of view head was used. This corresponds to a spot size of ~100 m when flying at 300 m above the ground.

[12] Aerosol samples on polycarbonate filters were collected through a small gas inlet on top of the aircraft. It is estimated that the 5 L per minute flow rate through the inlet was within ±20% of an isokinetic value. Samples were subjected to single particle analysis by a scanning electron microscope (SEM) with Energy Dispersive Analysis with X-rays for elemental qualitative analysis of C, O, and Na through Cu. Results of these analyses are given by *E. A. Reid et al.* [2003]

[13] Airborne particle measurements were made with two particle measuring systems (PMS) probes mounted on the Navajo wingtips (the Forward Scattering Spectrometer Probe and the Passive Cavity Aerosol Spectrometer Probe, or FSSP-100X and PCASP-100X, respectively). Both the FSSP and PCASP had undergone the Droplet Measurement Technologies Inc. upgrade to SPP-100 and SPP-200 signal processors, respectively.

[14] The PCASP measured particle sizes in 20 channels from 0.1 to 3 μm. The instrument was calibrated several times during the mission with polystyrene spheres (n = 1.59), and results are given by *J. S. Reid et al.* [2003]. Calibrations suggested that a static size binning was acceptable. Particle sizes were adjusted slightly to an assumed particle index of refraction of 1.5, which altered particle binning by <5%. During the mission the PCASP was operated with its deicing heaters on. This along with ram temperature increases the sample temperature by >10°C. Scattering cavity temperature measurements suggest this should have dried particles to <40% relative humidity.

[15] The coarse mode aerosol concentration was measured by the FSSP-100 in 20 bins with a nominal size range of 0.75 to 18 μm in diameter. Calibrations occurred alongside the PCASP and are given by *J. S. Reid et al.* [2003]. As discussed by *Collins et al.* [2000], the FSSP-100 is insensitive to particle size in 1 to ~15 μm range due to inflection points in the Mie size-scattering cross section curves. To account for this *Collins et al.* [2000] rebinned the FSSP data into three broad bins. However, intercomparisons with other particle sizing instruments performed by *J. S. Reid et al.* [2003] suggest that rebinning does not alleviate the problem and that interpreting size histograms from the FSSP (particularly for dust particles) is complex. While Reid et al. discusses the issue at length, a brief synopsis is presented here.

[16] Because dust is such a heterogeneous mix of various shapes and indices of refraction the response curve is no longer one to one. This problem is seriously aggravated by the presence of a Mie inflection point in the response curve for particles in the 4 to 10 μm range (which happens to be where most of the dust mass is located). While total particle counts and some very coarse sizing can be performed, the higher moment distributions for dust produce unphysical results. For example, the volume distribution for the FSSP yields particle volumes more than an order of magnitude too high compared to direct mass measurements at the surface. This uncertainty diminishes for the surface area distribution (factor of two too high). The number mode is probably more accurate. On the basis of regression correction with University of Miami instrumentation at the Cabras Island site, the FSSP can reasonably estimate dust particle mass (within ±25%). Further, ratioing of the smaller channels with the larger ones can be used to detect variance in the dust size distribution. The ratio of FSSP channels 2 + 3 with all of the remaining large particle channels appears to be the most sensitive.

[17] In this paper we utilize the FSSP data in ways that will minimize these errors and artifacts. As is typical with optical particle counters we exclude the first and last channel from our analysis, leaving a size range between 1.5 to 17 μm. We plot vertical profiles of the number concentration for FSSP channels 2 + 3 and channels 4 through 19 which correspond to roughly 1.5–3 and 3–17 μm, respectively. We are reasonably assured that these are independent size bins (i.e., no significant size errors), and this allows some qualitative feel for shifts in particle size with altitude. We also estimate dust particle mass concentrations as a function of altitude based on regressions from *J. S. Reid et al.* [2003]. This regression was developed by comparing the measured FSSP size distribution to the mass concentrations measured by the University of Miami. We estimate that these mass estimations have a ~25% absolute uncertainty. Finally, we provide vertical profiles of size ratios between particles roughly in size between 1.5 to 3 um and the 3–6, 6–11, 11–14, and 14–17 μm sizes. While *Reid et al.* [2003b] suggests that measurements of particle sizes in these bins are not necessarily independent, ratioing particle counts in the 1.5–3 μm and large size bins can qualitatively show if the size distribution of dust particles is changing with altitude.

3. AERONET Sun Photometer and MPLNET Lidar

[18] Two Aerosol Robotic Network (AERONET) Sun photometers were deployed on Puerto Rico for the PRIDE campaign. The principal Sun photometer was at the Cabras Island ground site at Naval Station Roosevelt Roads for the duration of the study (latitude 18.21°N, longitude 65.60°W). The second, installed on 1 July 2000, is still operating at La Paguera on the southwest corner of Puerto

Rico (18.0° N, 67.0° W). Data from the established Barbados site (13.2°N, 59.5°W) in the Caribbean and the Capo Verde (16.75°N, 22.9°W) and Dakar (14.4°N, 17.0°W) sites on the west coast of Africa are also used in this analysis [*Smirnov et al.*, 2000b; *Tanré et al.*, 2001]. The AERONET Sun photometers measured spectral aerosol optical thickness (AOT, τ_a) at six wavelengths (340, 380, 440, 670, 840 and 1020 nm) plus column-integrated water vapor from the 940 nm channel [*Holben et al.*, 2001]. The African and Barbados sites have polarization channels and measure optical depth at only 440, 670, 870, and 1020 nm plus water vapor. Optical depth data were collected every 15 min. Data were cloud screened and quality assured according to *Smirnov et al.* [2002a].

[19] Measurements of the vertical distribution of aerosols and clouds were made using a micro-pulse lidar system, or MPL [*Spinhirne et al.*, 1995]. The MPL measurements were carried out by the NASA MPLNET project [*Welton et al.*, 2001]. The MPL was installed inside the University of Miami aerosol trailer on Cabras Island, Puerto Rico. Continuous measurements were conducted from 28 June to 24 July 2001, except for ±1 hour of solar noon and occasional power outages.

[20] The MPL is a compact and eye-safe lidar system capable of determining the range of aerosols and clouds by firing a short pulse of laser light (523 nm) and measuring the time-of-flight from pulse transmission to reception of a returned signal. The returned signal is a function of time, converted into range using the speed of light, and is proportional to the amount of light backscattered by Rayleigh scattering, aerosol particles, and clouds. The MPL achieves ANSI eye-safe standards by sending laser pulses at low energy (μJ) and expanding the beam to 20.32 cm in diameter. A fast pulse-repetition-frequency (2500 Hz) is used to achieve a good signal-to-noise, despite the low output energy. The MPL has a small field-of-view (<100 μrad) and signals received with the instrument do not contain multiple scattering effects.

[21] The MPL signals are stored at 1-min time intervals, with a range resolution of 0.075 km from sea level up to a maximum altitude of 20 km. The raw data were converted into uncalibrated lidar signals, Normalized relative backscatter (NRB), using procedures discussed by *Campbell et al.* [2002] and *Welton and Campbell* [2002]. The NRB signals were then analyzed to produce profiles of aerosol extinction and optical depth, and the layer averaged extinction-to-backscatter ratio, using techniques discussed in the appendix of *Welton et al.* [2002].

4. Results

4.1. Mean Meteorology of the Region

[22] To put the PRIDE results into perspective it is necessary to consider the meteorology of the region and how the meteorological conditions during the study compared to other years.

4.1.1. Synoptic Situation

[23] The National Center for Environmental Prediction (NCEP) reanalysis fields [*Kalnay et al.*, 1996] for July 2000 were used to compare conditions during the PRIDE observational period to the long term mean (1948–2002). Despite the relatively coarse resolution of these fields, *Fyfe* [1999] has shown that this data set adequately represents the synoptic scale features of the region, including tropical easterly wave structure and propagation.

[24] Precipitation estimates based on a blend of outgoing longwave radiation (OLR) anomalies, SSM/I data, and rain gauge data [*Janowiak and Xie*, 1999] indicated that for 2000 there was a significant reduction in precipitation during the spring and early summer season in the northeast Caribbean, extending eastward across the subtropical Atlantic to the western Sahel. In July, negative anomalies of 25 to 50 mm below normal were observed in the northeastern Caribbean (30–40% below average), and 75–150 mm deficits in the west Sahel (50–100% below average). Positive anomalies occurred on the order of 150 mm in the Gulf of Guinea and northeast coast of South America (75% above average). Reynolds sea surface temperature (SST) anomalies [*Reynolds and Smith*, 1994] indicated colder than average SSTs on the order of −0.2 to −0.5°C extending from 5°N to 20°N across the entire Atlantic beneath the main dust track, with opposite warm anomalies of the same magnitude along the equatorial and midlatitude western Atlantic. In the area of the Atlantic High (20°–40°N, 30°–60°W), negative surface pressure anomalies of 2 mb and height anomalies aloft of 10 m existed below 700 mb, and conversely, positive anomalies of the same magnitude persisted in the middle and upper levels. Winds from the surface to 600 mb were 5–10 m s^{-1} stronger than average with a stronger northerly component.

[25] Increased synoptic stability due to reduced surface heat and moisture flux with ridging aloft is a likely mechanism for the observed positive outgoing long-wave radiation anomalies and reduced rainfall in the subtropical Atlantic discussed above. It is also proposed that the observed anomalous northerly component of the trade winds resulted in mean movement of tropical easterly waves farther south contributing to observed wetter conditions along the equatorial Atlantic and Brazilian coast, as well as contributing to the abnormally dry conditions in the Caribbean. The 600 mb composite winds and zonal anomaly for July (Figure 3) show that the observed patterns are consistent with findings by *Grist* [2002] and *Grist et al.* [2002] that the African Easterly Jet (AEJ) (5°–15°N, 10°W–20°E) shifts farther southward and is slightly stronger in dry Sahel years. This results in weaker amplitudes for easterly wave disturbances, resulting in weaker wave-associated convective precipitation.

[26] Figure 4 depicts observed rainfall for Tambacounda, Senegal, and Ouagadougou, Burkina Faso. Despite generally dry conditions in northwest Africa, stations in Burkina Faso and Benin in the ascent region of the midlevel easterly jet (MLEJ) and near the maximum cyclonic curvature, showed positive precipitation anomalies. This indicated that the principal precipitation band over Africa was further south than the climatological average. *Giannini et al.* [2000] found that cool subtropical Atlantic SST and anomalously dry Caribbean summers are often associated with a cold ENSO phase and a positive sea level pressure (SLP) anomaly in the North Atlantic High the previous winter. Although the observed ENSO cold phase was consistent in this case, below normal SLP was observed in the North Atlantic High during the 1999–2000 winter, which *Giannini et al.* [2000] correlated with wet (rather than the

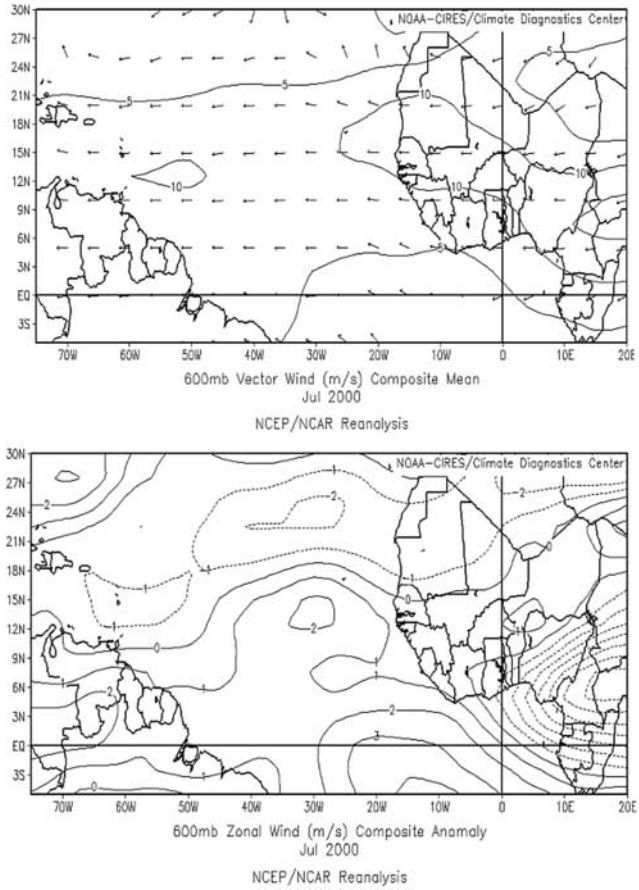

Figure 3. NCAR/NCEP reanalysis of 600 mb July 2000 mean wind vector field and zonal wind anomaly.

observed dry) conditions in the northeastern Caribbean the following summer.

[27] This meteorological situation in the subtropical Atlantic Ocean during PRIDE likely had a noticeable influence on dust production and transport into the Caribbean region. First, as easterly waves coming off of Africa are weaker than usual, we would expect lower winds and hence less dust production in Africa despite the negative precipitation anomaly in the dust producing regions. Second, *Karyampudi and Carlson* [1988] reported the AEJ, or midlevel easterly jet (MLEJ) as the Atlantic extension of this feature is called, occurs on the southern flank of the SAL and is associated with a direct transverse/vertical circulation and equator-ward ascent due to the enhanced baroclinicity between the warm dry Saharan Air Layer (SAL) and cool moist equatorial air. Hence as the MLEJ was much further south than usual for the region, we expect the center of the dust plume to also be further south than what is typical.

4.1.2. Local Conditions in Puerto Rico

[28] Typically in Puerto Rico fair weather trade cumulus were prevalent throughout the day. Morning cumulus usually gave way to clearer skies by noon. An example of a midday GOES image is presented in Figure 1b. Partially obscured skies would occur in mid to late afternoons due to cirrus blow-off from thunderstorms forming on the western side of the island in the lee of the central cordillera. Conditions were predominantly conditionally unstable, typically with convective lines (referred to as ''streamers'' by local forecasters) forming in the lee of smaller islands.

[29] Six easterly waves passed through the region during the study period, with wave passage occurring on ~28 June and 2, 7–8, 12, 14, and 18 July. Only the waves on 7 and 12 July caused significant precipitation or convective activity in Puerto Rico, and these passed within 6–12 hours. Because convection associated with the axis of easterly waves usually passed south of Puerto Rico during the study period, weather was more fair than what is typical during wave passage. The major changes were a wind shift and intensification and deepening of the easterlies during wave passage.

[30] Soundings from San Juan, Puerto Rico, depicting major atmospheric conditions of interest are presented in Figure 5. Figure 5a, from 21 July 2000 12:00 UTC shows a typical vertical structure during Saharan Air Layer (SAL) conditions. As reported by *Augstein et al.* [1974], the classic structure is a well-mixed marine boundary layer (MBL) extending from the surface to about 960 mb (500–700 m). Above this is a convective boundary layer (CBL) with fair weather cumulus clouds extending from the MBL inversion to the trade wind inversion at 750–850 mb (1500–2500 m). The SAL then extends from the trade inversion up to a small capping inversion at 500 mb (about 5000 m). The trade inversion height and strength can vary

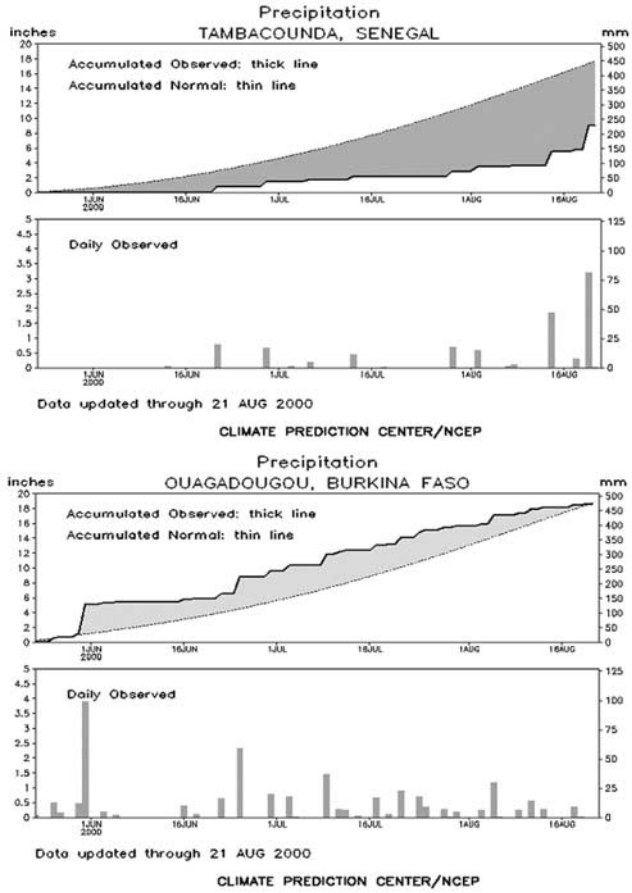

Figure 4. NCEP precipitation statistics for Tambacounda, Senegal, and Ouagadougou, Burkina Faso.

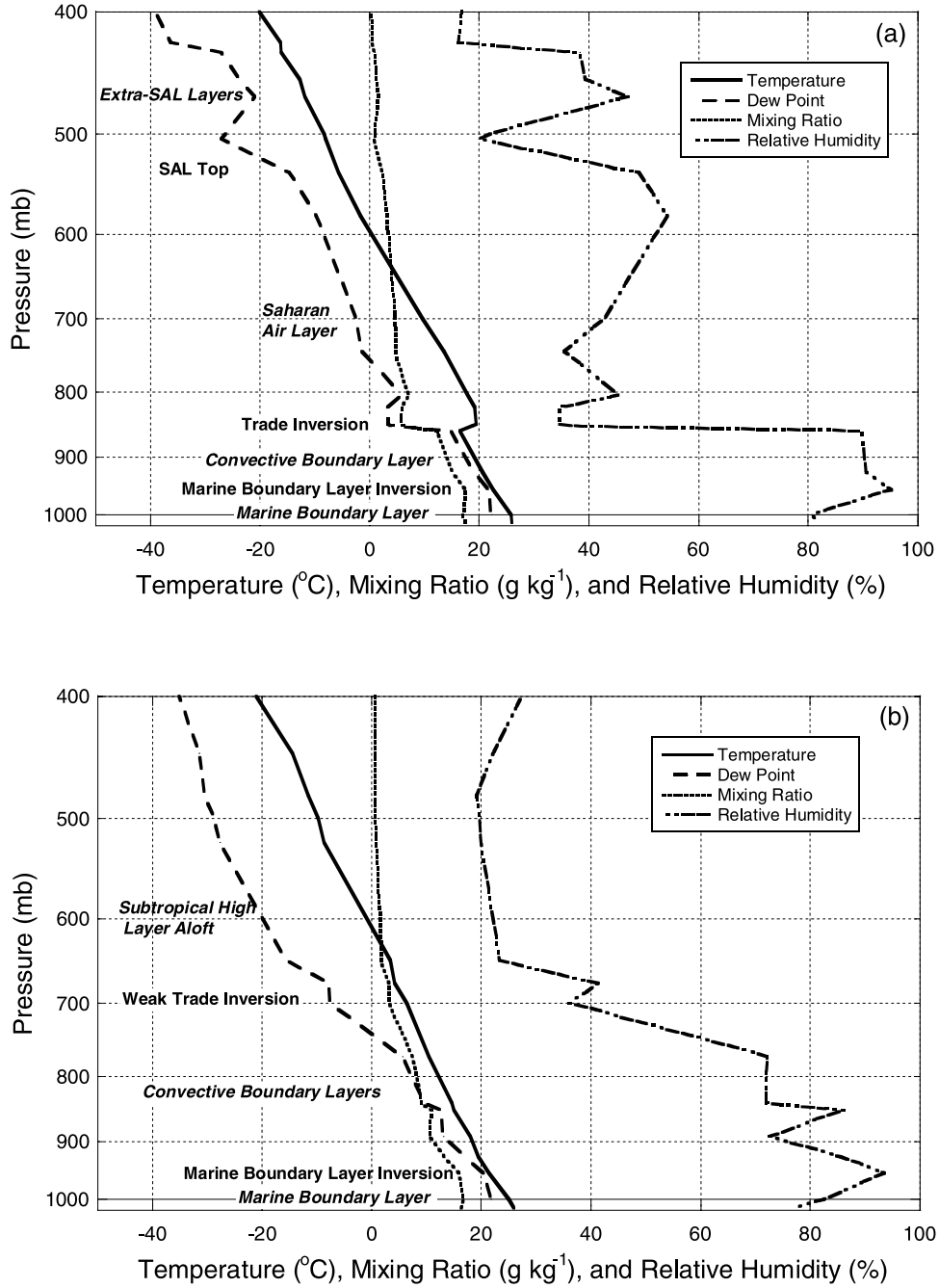

Figure 5. Example thermodynamic soundings from radiosondes released at San Juan Airport, Puerto Rico, for (a) 21 July 2000 the classic Saran Air Layer and (b) 7 July 2000 when the region was under the influence of easterly waves.

considerably from day to day, and even show a diurnal cycle on the order of ±250 m [*Augstein et al.*, 1974]. During strong "SAL" conditions the trade inversion was observed to lower to a minimum level of ~1 km and be as strong as 3°–4°C.

[31] Near the surface in the remote ocean environment, the dew point temperature is fairly close to the sea surface temperature. For the Caribbean, the sea surface temperatures and dew points ranged from 22° to 25°C, corresponding to water vapor mixing ratio (ω_v) values on the order of 17 to 23 g kg^{-1}. Above the trade inversion in the SAL, the air mass originates over land in Saharan Africa where strong sensible heating results in much lower dew points (below 5°C) with ω_v in the 3 to 6 g kg^{-1} range. The well-mixed MBL and the elevated SAL dictate the ω_v profile with relatively constant values in each region and a long gradient in the CBL due to convective mixing. Turbulent processes cause considerable fine structure not shown on this scale. The slope of the vertical ω_v gradient and shape of the ω_v vertical structure in the CBL indicates the degree of mixing occurring between the MBL and SAL through convective processes.

[32] When Puerto Rico was under the influence of an easterly wave, the trade inversion rose in altitude and weakened significantly. This left the lowermiddle troposphere very moist. An example is presented in Figure 5b with the 12:00 UTC 7 July sounding from San Juan, Puerto Rico. A cloud layer still forms at the top of MBL (here at ~950 mb). However, many additional cloud layers exist between the MBL and a very weak trade inversion at 700–650 mb. Above this weak inversion was a very dry subtropical high layer. The oscillation between SAL and easterly wave conditions was typically on the order of four to six days with the trade inversion gradually shifting in altitude and strength.

4.2. Optical Depths Over the African Coast and the Caribbean

[33] The NOAA AVHRR Pathfinder aerosol optical thickness composite for July 2000 is shown in Figure 1a. For the PRIDE period, dust dominated the 8° to 27°N latitudinal band across the Atlantic Ocean. Optical depths from the Pathfinder data suggested a July monthly mean value of 0.25 at Puerto Rico, and ~0.4 at the Cape Verde Islands just off of the African Coast (16°N, 24°W). The centerline sloped to the south slightly during transport, from approximately 20°N latitude at the coast of Africa (passing through the Cape Verde Islands) to ~17°N in the Caribbean (or ~1.3° south of Puerto Rico). The spatial distribution of the African dust was typical for the time period, and was within the 1989–1992 AVHRR climatology found by *Swap et al.* [1996b]. Despite the more southerly track of the easterly waves, the dust center for the 2000 season appears to be within the range of tracks observed by *Swap et al.* [1996b].

[34] Details on dust column loading can be found in the AERONET data from the region. Summary plots of data for Cape Verde, Dakar, Barbados, and Puerto Rico (a composite of the Roosevelt Roads and La Paguera sites) are presented in Figures 6a, 6b, 6c, and 6d, respectively. The most continuous record is from Cape Verde, with data available for most of the year. Dakar data were only intermittent with no data available for the winter and spring months. Similarly, the Barbados data were intermittent due to instrument failures. The Puerto Rico sites operated without incident from the study start date through the rest of the year.

[35] Despite the intermittent nature of the AERONET data set for these sites, examination of the data is insightful. Most importantly, for the year 2000 fairly typical dust temporal patterns were observed. Large dust events passed over Cape Verde and Dakar in all seasons. These events tended to be episodic in nature in the fall, winter and spring, but with a more sustained level in the summer months. From the Cape Verde data the largest events of 2000 occurred in the late winter and spring. Nine of the highest ten daily averaged optical depth days occurred outside the summer season.

[36] At the Caribbean sites, optical depths were low for most of the year with the exception of occasional strong and short dust episodes. At the Barbados site for the May, June, July, and August timeframe the commonly observed sustained summer dust feature appears with a maximum in June [*Prospero*, 1999; *Smirnov et al.*, 2000b]. The largest dust event of 2000 to remain coherent during transport into the Caribbean occurred in the last week of May, with large dust-falls being reported over much of the region, and Navy aircraft pilots operating throughout the region reported visibilities aloft <3 km. In Puerto Rico (after 28 June), the PRIDE field campaign appeared to have observed AOTs that were also typical for that season, with the dust falling off back to the episodic nature by 1 September.

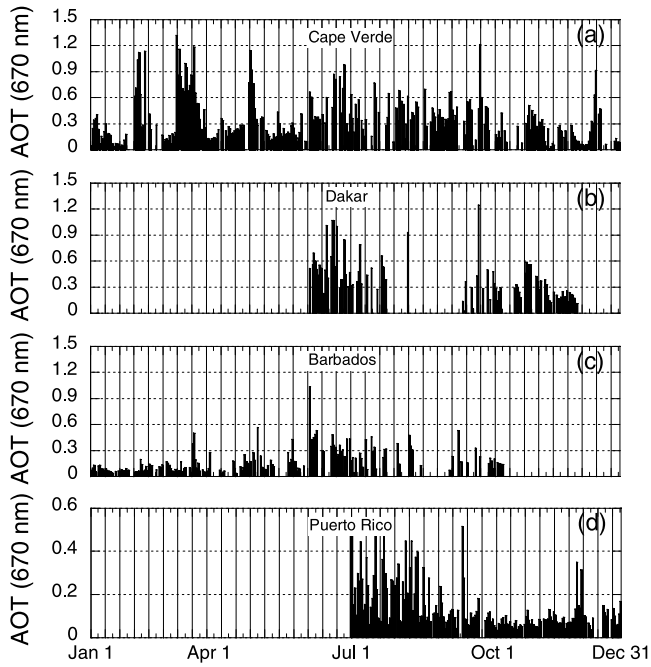

Figure 6. Year 2000 AERONET daily average aerosol optical thickness (AOT) at a wavelength of 670 nm measurements taken at (a) Cape Verde, (b) Dakar, (c) Barbados, and (d) Puerto Rico. The Puerto Rico data were taken from the Roosevelt Roads site during the PRIDE study period (until 24 July) and from the La Paguera site for the remainder of the year.

[37] While the 2000 dust season appears normal in its temporal characteristics, the anomalies in the mean meteorology of the region in 2000 (as discussed in section 3.1.1) may have manifest themselves in the amount of dust leaving Africa. Recall, the easterly wave track was further south than mean values, leading to a weakening of easterly wave activity. We would expect then a reduction in dust production over the season. The 670 nm daily averaged (± Std. Dev.) optical depths at Cape Verde for the May, June, July, and August timeframes were 0.22 ± 0.12, 0.52 ± 0.22, 0.38 ± 0.19, and 0.42 ± 0.14, respectively (note the July mean value of 0.38 is very close to the AVHRR Pathfinder value of 0.4 discussed above). These monthly averages are lower than the previous 4 years (but within a standard deviation). *Holben et al.* [2001] found over the 1996–1999 period daily mean AOTs averaged 0.4 ± 0.3, 0.7 ± 0.3, 0.6 ± 0.2, and 0.4 ± 0.2 over the months of May, June, July and August, respectively.

[38] Despite lower dust production and concentrations at the coast of Africa, dust concentrations in the Caribbean were more normal. Using the Barbados data as an indicator for dust transport into the lower Caribbean, the AERONET 670 nm mean AOTs were 0.16 ± 0.12, 0.34 ± 0.10, and 0.26

± 0.13, for the May, June and July 2000 timeframe, respectively (recall the Barbados site became more intermittent after July). These values are very near the 870 nm mean values for 1996–1999 given by *Smirnov et al.* [2000b] of 0.18 ± 0.10, 0.34 ± 0.22, and 0.24 ± 0.14, for May, June and July, respectively, 1996 to 1999 timeframe (Corrections for wavelength differences increase the Smirnov et al. values by no more than 0.03).

[39] Details of dust optical depths in Africa and the Caribbean during the PRIDE period can be found in Figures 7a, 7b, 7c, and 7d where daily average AOTs for the 20 June to 25 July period are displayed for Cape Verde, Dakar, Barbados, and Roosevelt Roads, respectively. The Roosevelt Roads data plot includes data from the La Paguera site for 3, 4, 22, and 23 July when no cloud screened data were available at Roosevelt Roads.

[40] During the PRIDE field campaign, Puerto Rico experienced 6 significant dust episodes, with peaks in AOT on 28/29 June and 5, 9, 15, 21, and 23 July 2000. Dust storms in Africa recurred roughly every 4 to 6 days. NAAPS and MATCH model runs suggest these events left the coast of Africa on 23/24 and 29 June and 4, 10, and 15/16 July (http://www.nrlmry.navy.mil/aerosol) [*Colarco et al.*, 2003] and can be corroborated qualitatively by available SeaWiFS data. The difference in the Puerto Rico and Cape Verde peak AOTs suggest a ~6 day transit time across the subtropical Atlantic Ocean. During the PRIDE field campaign, the average daily 670 nm optical depth at Roosevelt Roads was 0.25 ± 0.12. For the five peak dust days events at Puerto Rico, AOTs were 0.46 ± 0.11. Barbados had similar values with a mean 670 nm AOT value of 0.26 ± 0.12 and an average AOT of 0.40 ± 0.06 for the 5 highest days. Four of the five events observed at Puerto Rico were also seen at Barbados. Arrival times varied at Barbados but were usually within a day. High levels of dust were also found at Barbados on 13 and 23 July that were not seen at Puerto Rico.

[41] Figure 8a shows spectral AOT plots for three dust events plus a background day (AOT ~0.12) at Cape Verde. As is expected for coarse mode particles the wavelength dependence of the dust was spectrally flat. The 440–870 Angstrom exponent was fairly static with a study average of 0.24 ± 0.06. Such a low value suggests that at no time was the region significantly influenced by fine mode particles such as pollution from Europe, smoke from Africa or marine biogenic sulfate.

[42] Shown in Figure 8b are the daily average spectral AOT data for four dust events and clean marine days at Roosevelt Roads. Midvisible Angstrom exponents (440–870 nm) at this site were also low with study averages at 0.19 ± 0.11. On the 7 cleanest days with AOT < 0.1, the 440–870 nm Angstrom exponent increased only to 0.40 ± 0.13. Similar to the Cape Verde case, these values demonstrate that coarse mode particles (whether sea salt or dust) dominate the atmosphere's optical depth at Puerto Rico.

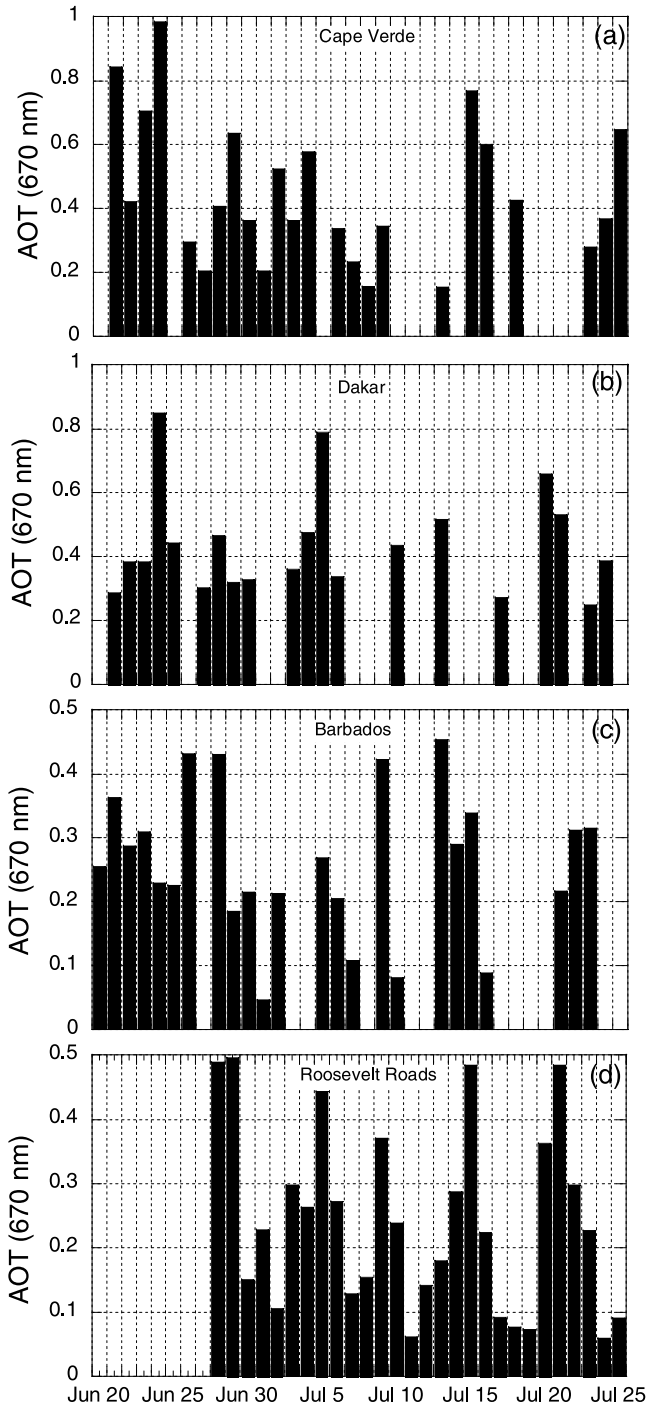

Figure 7. AERONET daily average aerosol optical thickness (AOT) at a wavelength of 670 nm measurements for the PRIDE study period. (a) Cape Verde, (b) Dakar, (c) Barbados, and (d) Puerto Rico.

4.3. Navajo Flight Operations

[43] Over the PRIDE field study, the Navajo performed twenty-one research flights for eighty flight hours. Data collection occurred for 61 of these hours. A summary of Navajo flight data collection times and atmospheric conditions is presented in Table 1. Flights occurred at least every other day, and typically began at 9:00–10:00 local Atlantic Time (13:00–14:00 UTC) in order to have the aircraft in position for the Terra overpass time of ~11:00 AM local time. The Navajo flew on 4 of the 5 heaviest dust days at Puerto Rico (the exception being 9 July).

[44] Each flight began with a continuous vertical profile from 30 m to ~5000 m over the Cabras Island aerosol/radiation site to characterize the local environment. If the

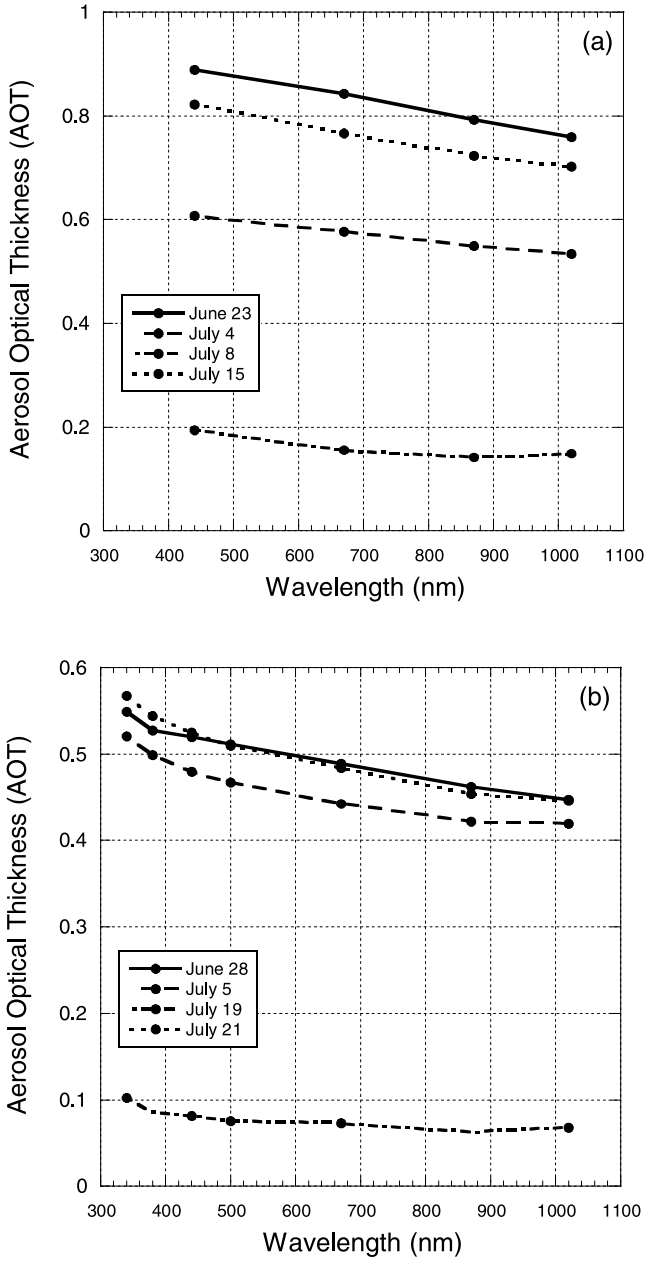

Figure 8. Aerosol optical thickness (AOT) as a function of wavelength for various days at (a) Cape Verde and (b) Roosevelt Roads, Puerto Rico.

site was totally cloud covered, we would move no more than 15 km to the southeast to find a cloud-free area. Once at altitude the Navajo proceeded to a cloud-free region 50 to 100 km away. In all but three cases this was in the region roughly bounded by Cabras Island, St. Croix (17°N, 65°W) and St. Thomas (19°N, 65°W). On 8 July, this region was heavily cloud covered and the aircraft flew offshore the west end of Puerto Rico. On 22 and 24 July, the aircraft proceeded south from Cabras Island 100 and 200 km, respectively, to sample heavier dust concentrations.

[45] Once at this secondary location the Navajo performed a descending profile to the surface. On selected flights intermittent level legs of ~10–20 km in length were included in the descent for making radiometer measurements. Once at the surface, the Navajo proceeded for 50 to 100 km in a generally north-south direction at 30 to 100 m altitudes to make optical depth measurements with the AATS-6 to validate Terra satellite products. The Navajo then either performed a final vertical profile to the top of the dust layer or returned directly back to Roosevelt Roads. By the end of PRIDE, the Navajo had performed 58 vertical profiles on 21 days.

[46] During the PRIDE study period, the Navajo took measurements in a variety of conditions, from days with very strong trade inversions and fair weather, to very moist atmospheres under the influence of easterly waves. As discussed in the PRIDE preliminary findings paper by *Reid et al.* [2002], we also found dust not only in the SAL layer, but in a wide variety of vertical distributions. In the following sections, we divide our measurements into three groups. First, we discuss days with very clean (little dust) background conditions. Second, we present data from observed dust events, which conform to the SAL dust transport conceptual model. Last, we examine days that have variable dust vertical distribution and do not fit into either classification.

4.3.1. Clean Marine Conditions

[47] On the 8, 11, 17, and 19 July flights, AOTs in the vicinity of Puerto Rico were below 0.08. These observed optical depths are consistent with clean and marine environments [*Smirnov et al.*, 2002]. As with other times during the study, Ångström exponents were low during clean periods at 0.47, 0.25, 0.34, 0.25 for the 8, 11, 17, and 19 dates, respectively, indicating that coarse mode salt particles dominated the atmospheric optical depth. At the surface, easterly trade winds were consistently in the 5–7 m s^{-1} range. Skies were mostly clear over the ocean for the 11, 17, and 19 July episodes, with <15% coverage by fair trade cumulus and occasional cumulus congestus. For 8 July, the region was under the influence of an easterly wave to the south, with a much more moist lower troposphere and 20% coverage of cumulus congestus, and >60% thick cirrus coverage. D. L. Savoie et al. (Vertical distribution of Saharan dust aerosols over the tropical North Atlantic based on ground-based dust measurements and AERONET aerosol optical depths, submitted to Geophysical Research Letters, 2003) (hereinafter referred to as Savoie et al., submitted manuscript, 2003a) found dry sea salt concentrations to be ~15–20 μg m^{-3} on these days, compared with dust concentrations <5 μg m^{-3} during the flight.

[48] Summary profiles of atmospheric conditions in Cabras Island region for background days can be found in Figure 9. In the first column, soundings of temperature (T), dew point (T_d), equivalent potential temperature (θ_e), and water vapor mixing ratio (ω_v) are presented. In the second, summary soundings of coarse mode particle concentrations and estimated coarse mode mass from the FSSP are presented. Number concentrations are split between the 1.5–3 μm and 3–17 μm ranges. To estimate mass concentration, the surface area-to-mass regression used by *J. S. Reid et al.* [2003] is utilized. In the third column, sounding plots from the PCASP are presented. Here the data are broken into two categories. First, the estimated mass of particles (assuming a density of 1.4 g cm^{-3}) less than 0.3 μm in diameter is given. These particles are not likely to be from aolian sources, but rather pollutants from Africa or

Table 1. Summary Flight Information for the SSC-SD Navajo[a]

Date	Data Collection Period, UTC	Number of Vertical Profiles	MBL Height, m	Trade Inversion, m	EH Inversion	Cabras Island Profile AOT	Estimated Dust Loading, g m^{-2}
28 June	13:15–15:00	2	450	1100	4100	0.48	0.55
30 June	13:00–16:30	4	550	1600	3700	0.24	0.23
1 July	13:00–16:15	3	750	2000	2500	0.13	0.08
3 July	14:30–17:00	2	450	1800	4100	~0.20	0.17
4 July	14:00–17:15	4	300	2000	4800	0.29	0.29
5 July	13:15–16:00	3	450	1900	4800	0.35	0.37
6 July	13:00–16:30	4	400	1000	4500	0.25	0.24
8 July	13:00–15:15	2	700	none	none	~0.06	<0.03
10 July	13:15–16:30	3	650	1600	3300	0.15	0.11
11 July	13:00–16:15	3	450	2800	3100	0.06	<0.03
12 July	13:00–16:15	3	800	2100	4000	0.12	0.07
13 July	13:30–17:00	2	500	1350	3000	0.17	0.13
15 July	14:15–18:00	3	500	1150	4800	0.26	0.25
16 July	13:15–16:15	3	800	1950	4000	0.23	0.21
17 July	13:00–14:30	2	500	2000	3000	0.07	<0.03
19 July	14:15–15:30	2	400	2100	3100	0.06	<0.03
20 July	14:15–17:00	3	500	2300	5500	0.27	0.27
21 July	13:15–16:15	3	600	1350	4950	0.35	0.37
22 July	13:30–16:00	2	500	1950	3800	0.11	0.05
23 July	12:30–16:00	3	200	1650	4200	0.30	0.31
24 July	13:15–16:15	2	450	2000	3900	0.15	0.11

[a]Profile aerosol optical thickness (AOT) is the difference between the AOT at the surface and the AOT at the Saharan Air Layer (SAL) top at 500 nm. EH inversion is the height of the extratropical high forming a dry supra-SAL layer. Estimated dust loading was approximated by subtracting the clean marine background AOT (0.07) from the profile AOT and then dividing by the average mass extinction efficiency of dust for PRIDE (~0.75 m^2 g^{-1} (Savoie et al., submitted manuscript, 2003a; D. L. Savoie et al., Spectrally-resolved light absorption by Saharan aerosols over the tropical North Atlantic, submitted to *Geophysical Research Letters*, 2003 (hereinafter referred to as Savoie et al., submitted manuscript, 2003b)).

secondary particles produced over the ocean. Also shown is the estimated mass concentration of particles in the 0.3 to 1.1 μm range, that are more likely to represent small dust particles and some sea salt (for dust we assumed an effective density of 2 g cm^{-3}).

[49] All of the background days studied had similar characteristics. The MBL from the surface to 500–700 m was clearly evident from the constant values of θ_e and static values of ω_v at ~18 g kg^{-1}. Above the MBL was a deep, moist and neutral CBL that extended through several weak inversions up to a stronger one at 2000 to 3000 m. In the CBL, water vapor mixing ratio tended to monotonically decrease to a value of 10 g kg^{-1}. These conditions suggest that moist convective mixing was responsible for air exchange between MBL and aloft. Above the weak trade inversions were occasional ~1000 m deep layers topped by a strong subsidence inversion at 3000–4000 m. The layer defined by these last two inversions tended to have a ω_v of 2–10 g kg^{-1} and could have had continental origins or have been a remnant of a previous subsidence inversion. This may be considered a "SAL", but there is little dust in this layer (see below) the air dried rapidly with ω_v dropping to less than 1 g kg^{-1}.

[50] The fine and coarse mode particle vertical distribution peaks were bounded by the inversions. Both fine and coarse particle mass concentrations were at a maximum at the surface and MBL. Coarse mode sea-salt particles dominated the MBL with ambient concentrations increasing to a maximum at cloud base due to hygroscopic growth. Occasional brushes with clouds caused peaks in the FSSP number concentrations and mass at the MBL top. Since the PCASP measures dry size, it shows a falloff with altitude. There is large discrepancy in magnitude between the regression mass and 1.5–3 μm mass estimation in the FSSP, indicating the coarse mode is indeed dominated by large sea-salt particles. Between the weak inversions of the CBL some thin layers of both fine and coarse mode particles are observable, however the concentration of coarse mode particles fell to below detectable limits at 2000 m.

4.3.2. Strong SAL Conditions

[51] Only over the last five days of the PRIDE study (20–24 July) did we observe dust vertical distributions that were considered "typical" for Saharan dust transport into the Caribbean. Vertical sounding plots for 20, 21, 22, and 23 July flights are presented in Figure 10. The case on the 24 July (not shown) was very similar to that of 22 July. As with most of the clean marine days, local weather during this period was fair, with scattered trade cumulus over the oceans and afternoon thunder storms developing on the west side of Puerto Rico.

[52] As discussed in section 4.3.1, 19 July could be considered a clean marine background day with minimal dust detected. On the late evening of 19 July, the first signs of the dust event appeared at Puerto Rico. By the morning Navajo flight of 20 July, the profile midvisible AOT had increased from 0.06 to 0.27. A moist MBL and CBL was topped by a moderate trade inversion base at 2800 m. A SAL is evident from the sounding with a ω_v values being a static 3–5 g kg^{-1} in the 3000–5800 m range. Such a value is clearly from continental origins. If ω_v were lower, it would be too dry to be from Africa, and if higher, it would have indicated marine influence. The SAL is topped by a subtropical subsidence inversion at 5600 m. Particle soundings show a clear dominance of dust particles in the SAL between 2300 and 4500 m (note that the top of the dust layer is lower than the top of the SAL). Distinct layering is also visible at 3500 and 4200 m. An additional thin particle layer is also visible in the 4800–5600 m region.

[53] Atmospheric dust is best seen in the FSSP 1.5–3 μm and PCASP 0.3–1.1 μm data. These particles are generally

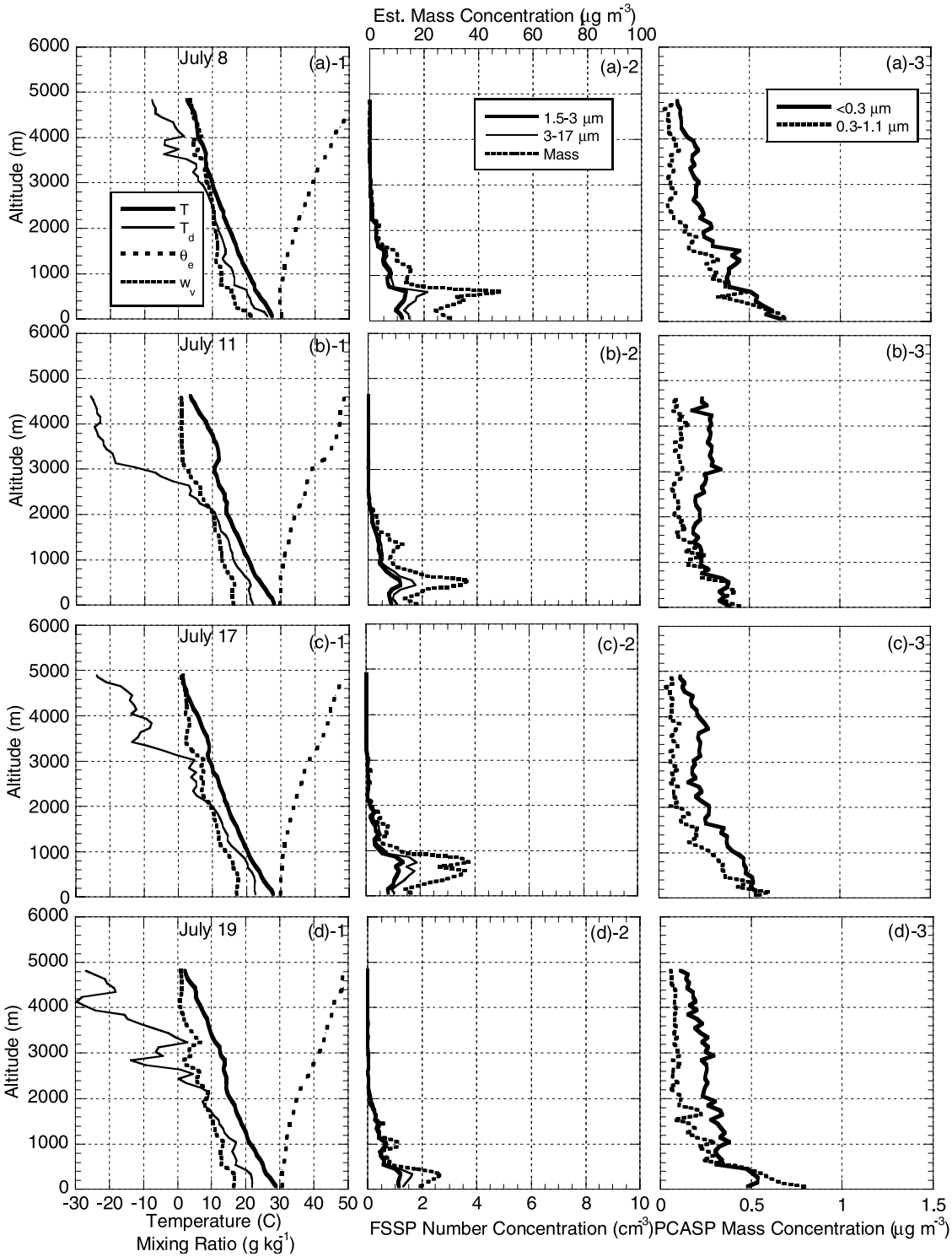

Figure 9. Atmospheric soundings from the Navajo aircraft for four days with clean marine conditions (8, 11, 17, and 19 July 2000). First column, thermodynamic state variables temperature (T, thick solid lines), dew point (T_d, thin solid lines), equivalent potential temperature (θ_e), and water vapor mixing ratio (ω_v, tight dashed lines). Second column, FSSP number concentration (1.5–3 μm, thick solid lines; 3–17 μm, thin solid lines), and estimated coarse mode particle concentration (dashed lines). Third column, estimated fine mode mass concentration from the PCASP for particles <0.3 μm (solid lines) and 0.3–1.1 μm (dashed lines).

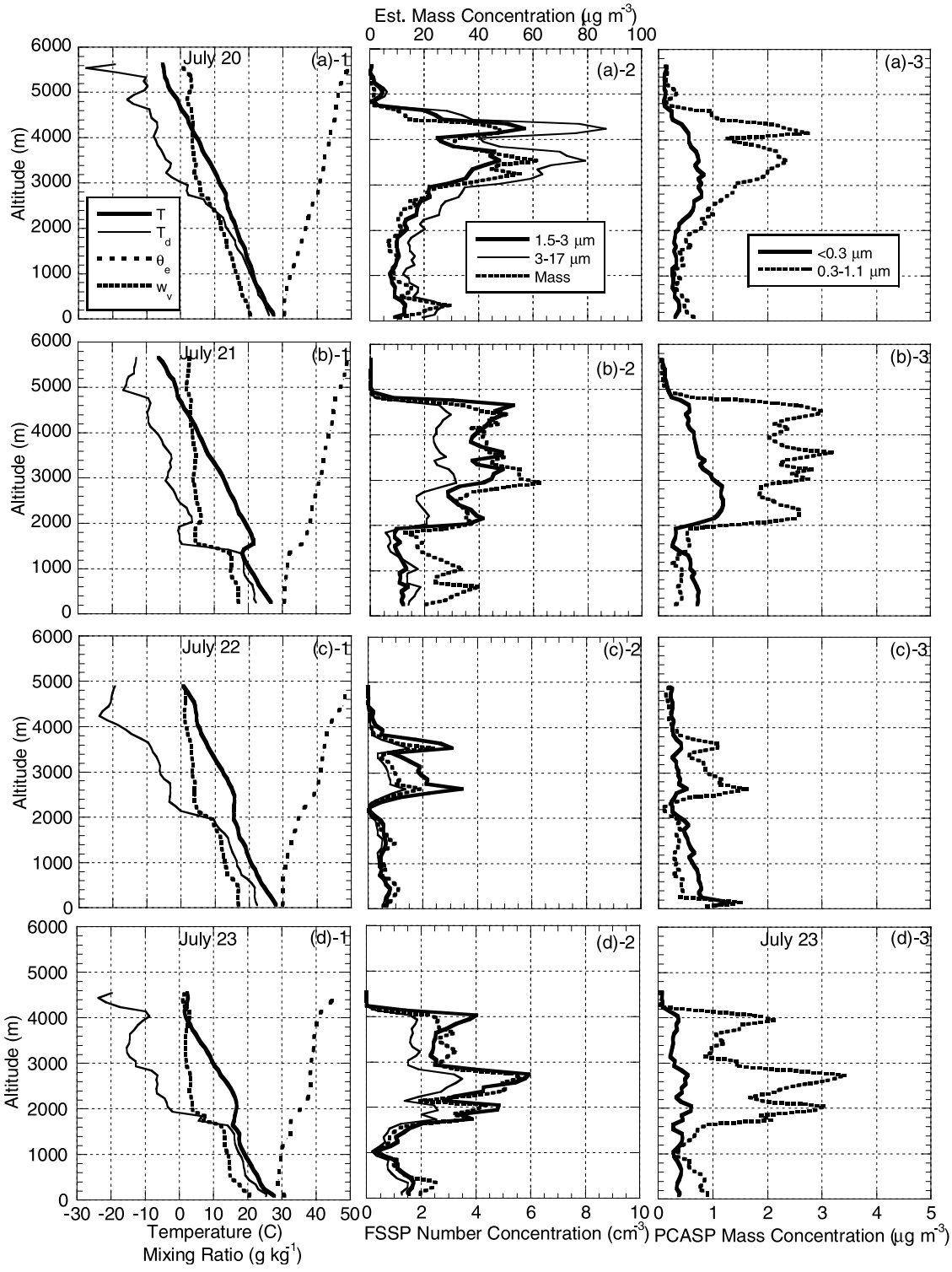

Figure 10. Same as Figure 9 but for four days with SAL transport conditions (20–23 July 2000). Note the scale change for column 3.

too small to be sea salt, and too large for accumulation-mode anthropogenic particles. Comparison of FSSP number concentration in the 1.5–3 and 3–17 μm ranges suggests that there are only slight shifts in particle size with altitude. A crossover does occur above 4600 m at the top of the dust layer. As counting statistics suggest that sufficient large dust particles were measured in the FSSP, this change in size is likely due to depletion of the larger dust particles at the very top by gravitational settling. The PCASP soundings in the 0.3–1.1 μm range followed the FSSP soundings very well, mirroring the layered structure, although some height differences exist. Since these particles do not have appreciable

fall velocities (~3 m per day for 1 μm particle), this PCASP data probably is the best tracer that describes the vertical distribution of dust without the influence of fallout. Comparisons of the particle mass in the PCASP and FSSP size ranges indicates a dominance of coarse mode particles (25:1 mass ratio) which is consistent with the small Angstrom exponents found at the AERONET Sun photometer site. While accumulation mode particles <0.3 μm do show a slight increase in the SAL it does not strongly mirror the layering structure of the dust. This increase might represent dust in combination with low concentrations of anthropogenic primary or secondary particles transported across the Atlantic Ocean with the SAL air mass. Regardless, large dust particles clearly dominate the atmosphere's light extinction and AOT.

[54] By the 21 July flight, dust optical depths reached a midvisible profile AOT of 0.35. AERONET and lidar data (discussed later) suggests this was in a temporary minimum in the dust down from 0.5 approximately 4 hours before and after the flight. For the flight period dust concentrations were slightly lower on 20 July, but the SAL was considerably deeper. On 21 July, the trade inversion had dropped to 1350 m and strengthened by 3°C. However, the well-defined trade inversion did not delineate the start of the dust layer in the SAL. A 500 m thick region with slightly suppressed ω_v values was relatively particle free. At 2000 m, a slight increase in dew point and w_v to 5 g kg^{-1} coincided with the increase in particle concentration within the SAL. Dust layering was also present on this day. Most of the shifts in particle concentration were accompanied with small shifts in w_v.

[55] Qualitatively, it also appears as if there is a shift in particle size distribution over the previous 24 hours. In Figure 10 (plot a-2) we find that the ratio of 3–17 μm to 1.5–3 μm particles on 20 July in the SAL was approximately 3:2. For 21 July (and all subsequent days), this ratio reverses, to approximately 2:3. As on 20 July, the clear upper level dominance in the concentration of dust is best seen in the FSSP 1.1–3 μm and PCASP 0.3–1.1 μm ranges. The accumulation mode particles in the PCASP (<0.3 μm bin) also show an increase in the SAL, but almost no layering is present. This again supports the presence of some anthropogenics. In the MBL and CBL, the FSSP regression mass values suggests some particle enhancement below the main dust layer. Filter measurements by Savoie et al. (submitted manuscript, 2003b) suggest roughly half of this increase is due to sea-salt.

[56] By 22 July, AOTs dropped significantly, to 0.11, but the dust was still the dominant species in the SAL. Over the previous 24 hours, the trade inversion weakened slightly and increased in altitude to 2000 m. The supra-SAL subsidence inversion also descended, leaving the dust in a layer only 2000 m thick. Further, fine mode particle concentrations were near the clean marine background conditions.

[57] Finally, on 23 July, the Navajo caught another pulse, and AOTs increased back up to 0.3. Here, the subsidence inversion remained at 4000 m, but the trade inversion descended to 1650 m. Of all of the days monitored, this day appeared to have the most stratification in dust. However, like the previous day, accumulation mode particles were extremely low in number and had little correlation with the dust.

4.3.3. Lower Level Dust Transport

[58] The dust events discussed in section 4.3.2 fit well with the *Karyampudi et al.* [1999] description of periodic summertime SAL dust outbreaks from Africa and corroborate the observations in the region by *Prospero and Carlson* [1972]. Dust was the dominant aerosol species above the trade inversion in the SAL with some layering present. The SAL was topped by a subtropical subsidence inversion, above which virtually no dust existed. On the basis of these findings, it would seem reasonable to estimate dust particle distribution based on atmospheric sounding profiles and an independent measurement of optical depth by confining most of the dust between the trade and subsidence inversions. However, in the first half of the PRIDE study, the dust vertical distribution deviated considerably from the conceptual model.

[59] Figure 11 shows Navajo vertical profile data over the Cabras Island for four days at the beginning of the study. The very first day of the mission, 28 June, had the highest optical depth of dust during a Navajo flight. Skies were ~50% cirrus covered, but profile bottom AOTs in clear patches were on the order of 0.5 [*Livingston et al.*, 2003]. Subtracting the mean of clean marine days, this implies dust AOTs were on the order of 0.41. At times, reported visibility by aircraft in the region dropped below 6 km during the day. Indeed, the island of Vieques, 10 km away from the Cabras Island site, was only barely visible at times. Filter sampling had not started during the study yet, but based on Navajo FSSP and PCASP data we estimate that dust concentrations at the surface were at least 100 μg m^{-3} during the flight. On the basis of visibility reports, the dust concentration at times must have been several times greater.

[60] The dust vertical distribution and atmospheric sounding for 28 June was unlike any other during the study. Like the 21 July SAL case, the trade inversion was strong and relatively low at 1100 m. The upper level subsidence inversion was lower than the 21 July case by ~1000 m, confining the dust to altitudes below 4000 m. What was remarkable about the sounding however, was that the atmosphere was relatively dry below the trade inversion. In all other flights during PRIDE, w_v values were ~18 g kg^{-1} throughout the MBL, typical for the tropics. For the 28 June case ω_v was 18 g kg^{-1} at the surface, but decreased rapidly to ~12 g kg^{-1} by 500 m- thus indicating that the MBL was not well mixed. Further, the cloud base was not at ~500 m as it was in previous days, but rather it was at the trade inversion itself. Above the trade inversion a SAL was clearly evident with ω_v constant at the expected value of 5 g kg^{-1}.

[61] Both the FSSP and PCASP soundings indicate that, contrary to what is assumed, dust reached maximum concentrations below the trade inversion. In the SAL, the FSSP suggested the dust concentration was on the order 50 μg m^{-3} or slightly greater than the SAL case days shown in section 4.3.2. Below the trade inversion, values reached 100 μg m^{-3}. As was typical, particle volumes of large particles increased at cloud base due to deliquescence and occasional cloud droplets. The increase was not as substantial in the 1.1–3 μm bin and the PCASP data.

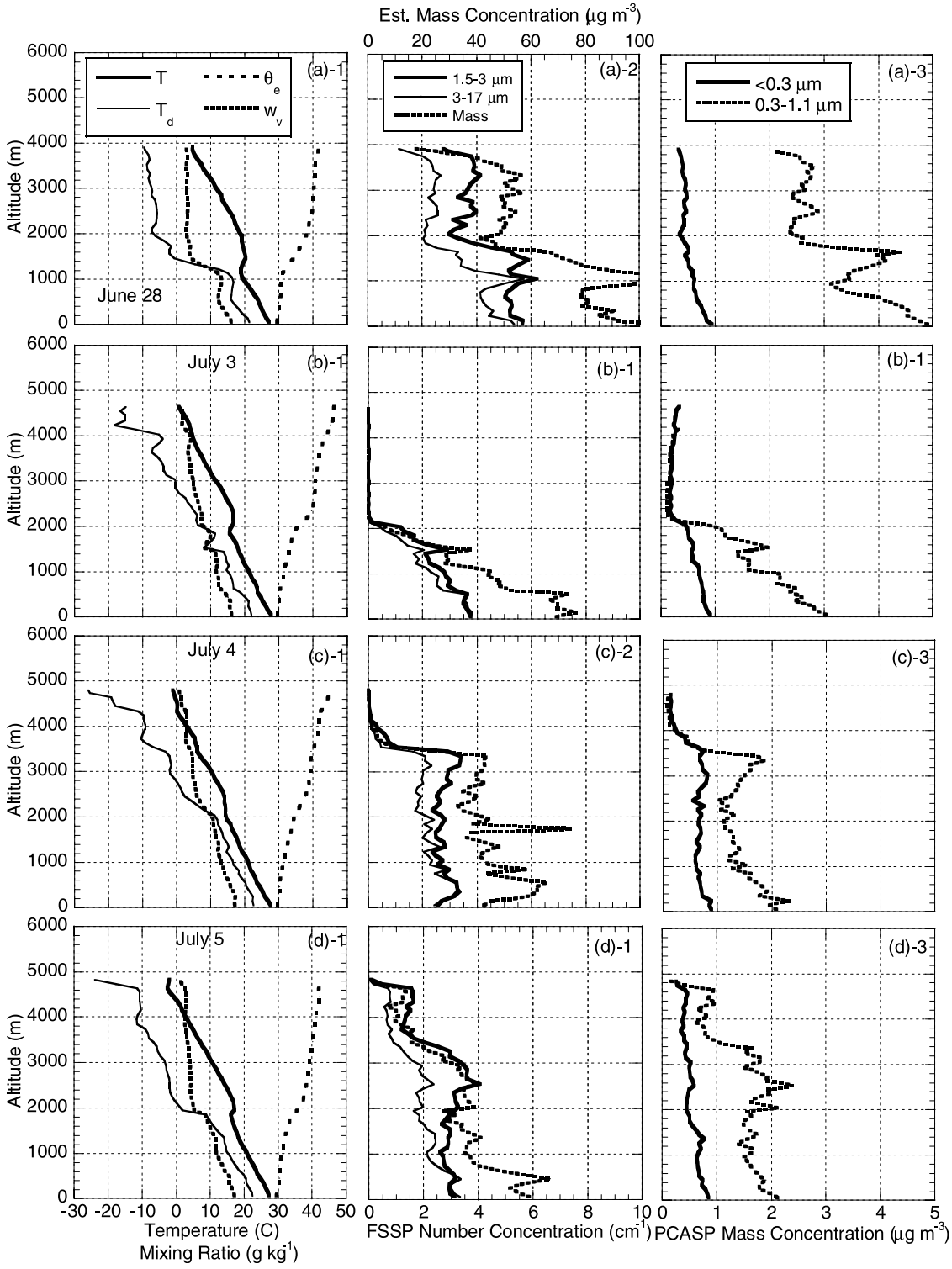

Figure 11. Same as Figure 9 but for four days the first week of the study when dust was dominant below the trade inversion (28 June and 3, 4, and 5 July).

[62] On the days following this large event, dust vertical distributions varied considerably. On the 3 July flight (Figure 11b), which exhibited a weak trade inversion at 2000 m, dust was strictly confined below the trade inversion, despite the presence of an obvious SAL layer between 2000 and 4000 m. For the flight on 4 July (Figure 11c) and 30 June flight (not shown), dust was evenly distributed throughout the CBL and shallow SAL with slight maximums at the very top of the SAL and at the surface. On 5 and 6 July flights (not shown) a strong trade inversion had developed at 2000 m, but dust concentrations still appeared to be constant across the inversion.

This is similar to the vertical distributions shown by *Prospero and Carlson* [1972] for the May–June time period during the BOMEX study, but with considerably higher concentration.

[63] Clearly, there was a shift of dust vertical distribution between the beginning and end of the PRIDE study. This shift occurred for the most part without significant changes in the atmospheric thermodynamic sounding (with the exception of 28 June and the very strong SAL on 21 July.). The shift from "mixed" or "low level" transport to the more classic "SAL" transport did not happen suddenly, but rather over a period of 10 days. Figure 12 presents four flight soundings during this transition period. Like previous days, on 10 July a SAL was present, although the subsidence inversion was lower at 3500 m. Trade cumulus clouds were scarce, with the only clouds being from streamers coming off local islands. Using the 1.5–3 μm and PCASP 0.3–1.1 μm channels as an indicator of dust, the vertical distribution is somewhat bi-modal, with dust maximums in the SAL and in the MBL and a clean layer in between. Despite higher optical depths the previous day (9 July), 10 July had the highest mass concentrations measured by a surface sampler during the study [*E. A. Reid et al.*, 2003]. By 13 July, the bimodal nature becomes more pronounced. By 15 July, the dust appears to have shifted into the SAL transport pattern with most dust above a strong trade inversion at 1100 m. As the atmospheric dust loading began to decrease on 16 July, a SAL dust layer was evident from 2000 to 4000 km, and a separate lower level dust layer was found in the MBL with concentrations rivaling those aloft. In fact, despite the decrease in dust AOT between the two days (daily average AERONET AOTs of 0.48 to 0.24 for 15 and 16 July, respectively) the 24-hour filter samples taken by Savoie et al. (submitted manuscript, 2003a) show a mean increase in surface dust concentration from ~30 to ~50 μg m^{-3}.

4.3.4. Regional Dust Variability

[64] During the PRIDE study we typically did not detect much variability in the dust vertical distribution in the Puerto Rico region on the multiple vertical profiles of each Navajo flight. This is probably in part due to the limited range of the aircraft on most days. However, there were several occasions when the gradient of dust was so strong that it was easily detectable. The four strongest cases are presented in Figure 13, where we present the atmospheric temperature and dew point sounding, FSSP particle concentration in the 1.5–3 μm range, and the aircraft flight track overlaid on the GOES 8 visible image from the beginning of the flight.

[65] Variability in dust properties took several forms including uniform shifted in height and/or concentration. Consider 5 July (Figure 13a), where three vertical profiles were taken at Cabras Island, St. Croix, and St. Thomas. In this case very similar atmospheric soundings with a moderate trade inversion at ~1800 m and a supra-SAL inversion at 4800 m were observed. For the St. Croix case, the sounding indicates the CBL to be slightly more moist, but this could be due to very localized effects (e.g., flying closer to a cloud). Particle soundings however show more variance. While the Cabras Island and St. Croix vertical profiles are very similar, the profile taken 10 km south of St. Thomas shows about a one-third reduction in particle concentrations uniformly with height. For example, the thin layer between 3800 and 5000 m and the minor maximum at 2800 m are reproduced in all three soundings.

[66] Other gradient days showed more variation in vertical structure of the dust, although for the most part the atmospheric thermodynamic soundings stayed fairly static. Consider the 10 July case (Figure 13b), which showed the strongest gradients of any flight of the study. After the initial vertical profile from Cabras Island (AOT = 0.15), the Navajo proceeded to a point ~50 km north of St. Thomas where midvisible dust AOTs increased to 0.2. After completing a descending profile, the Navajo flew south ~120 km to a point west of St. Croix, where AOTs dropped to 0.12. These changes in AOT were coupled with vastly differing dust vertical profiles. At Cabras Island, dust was fairly uniformly distributed from the surface to 2200 m and then monotonically fell off. North of St. Thomas, the dust vertical distribution was more typical for SAL transport with a peak in dust concentration aloft, although there was still some dust enhancement in the MBL and CBL. After flying south to the lowest AOT region, we find the dust has kept its more SAL transport-like nature, with a peak in dust concentrations aloft. However, here we find the SAL dust layer considerably thinner. Accompanying this change is the presence of a very moist layer at 2700–3300 m, most likely due to cumulus outflow.

[67] The 22 July case also had its own character. On this flight soundings were taken at Cabras Island and 120 km south at ~17°N latitude. Optical depths increased from 0.11 to 0.22 between these two points. Like other days, the trade inversion, CBL and MBL were nearly identical. The most significant difference in the thermodynamic sounding was an increase in the supra-SAL subsidence inversion as we moved south from 3800 to 4200 m and the subsequent deepening of the SAL. While the prominent layer structure remained the same between both locations with uniform increases in amplitude, we find a systematic shift in layer height by about 300 m. These shifts in dust layer altitude logically corresponded to equivalent shifts in water vapor mixing ratio: a natural tracer for the dust.

[68] Finally, on 24 July, we flew the furthest from Puerto Rico than in any other part of the study. After completing the Cabras Island sounding (AOT = 0.15), the Navajo flew south to the 16° latitude point (~170 km) where midvisible optical depths increased to 0.22. This day demonstrated a tremendous amount of layering over the Cabras Island site with dust dominant in the SAL. Further south, this layer gave way to a more uniform dust distribution, with higher dust concentrations below the trade inversions in the CBL.

4.3.5. Dust Particle Size Issues

[69] Dust particle size distributions are presented by Savoie et al. (submitted manuscript, 2003a), *E. A. Reid et al.* [2003], and *J. S. Reid et al.* [2003] from many aerodynamic, geometric, optical and inversion methods. A "best fit solution" is lognormal with a volume median diameter of 3.5–5 μm and a geometric standard deviation of 1.9–2.2. However, these studies also show that as dust is a mix of particles with complicated shapes and chemistries, size distributions such as these are difficult to apply. While in this study we are not concerned with the mean dust size

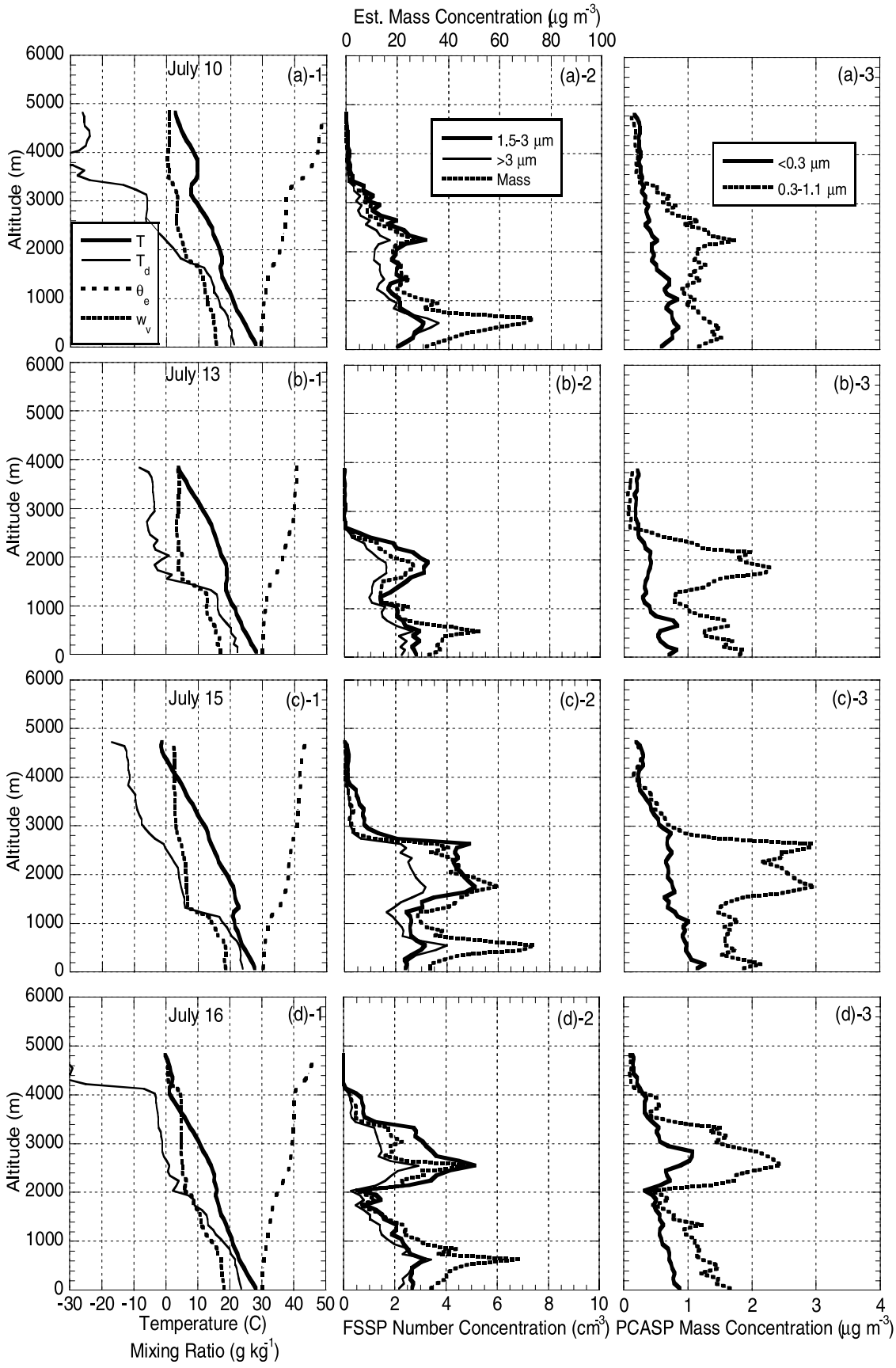

Figure 12. Same as Figure 9 but for the middle of the study when dust was in transition between lower level and SAL transport (10, 13, 15, and 16 July).

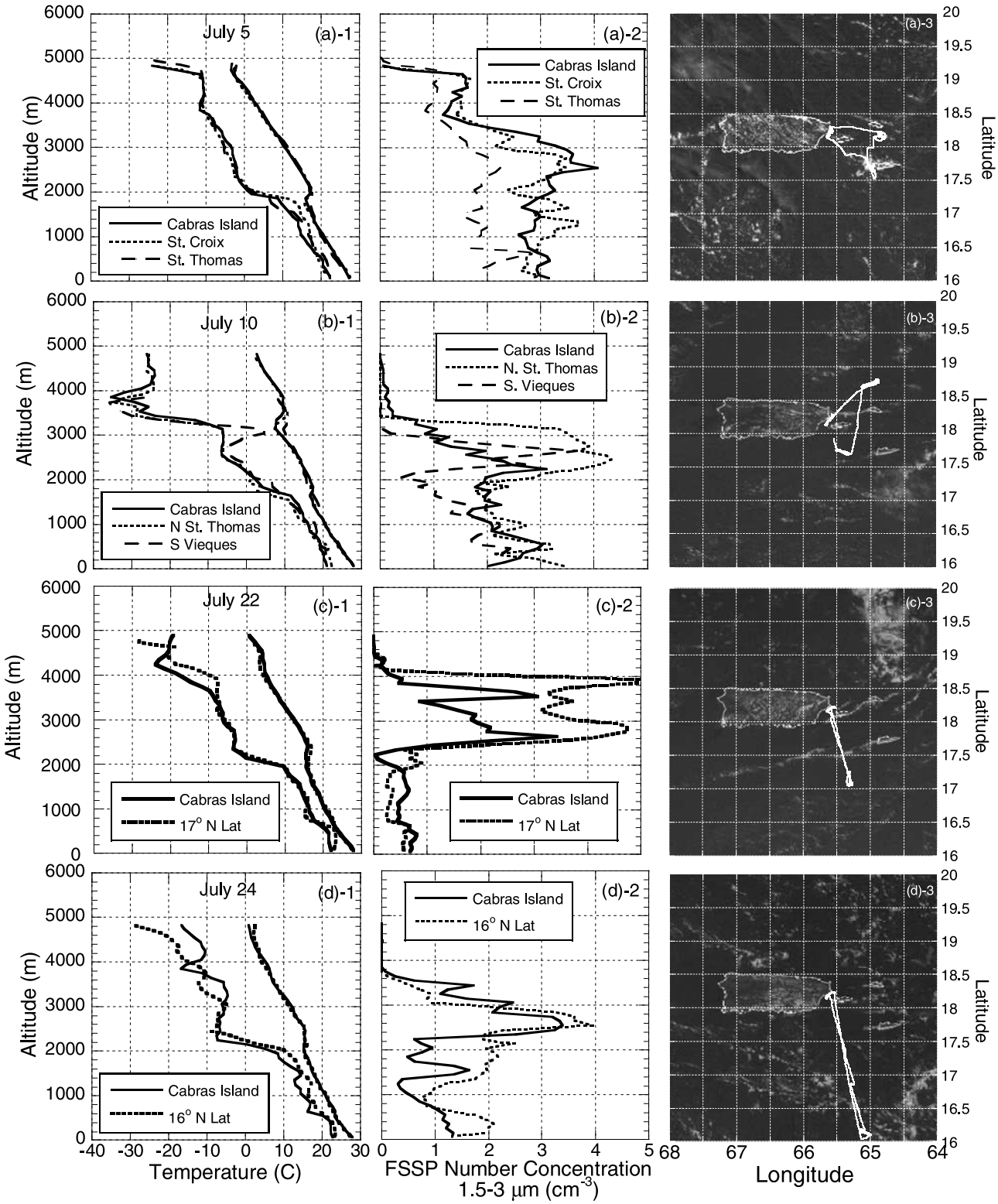

Figure 13. Atmospheric soundings from the Navajo aircraft for four days when a gradient was seen in dust concentrations and vertical profiles. (5, 10, 22, and 24 July 2000). First column, temperature and dew point. Second column, FSSP number concentration (1.5–3 μm, thick solid lines; 3–17 μm, thin solid lines), and estimated coarse mode particle concentration (dashed lines). Third column, GOES 8 image taken at flight time with flight track overlaid.

distributions, we are interested in how these may be changing with height. Over the course of the PRIDE field study, we did not detect any dramatic shifts in particle size from day to day. This is in part due to the insensitivity of the wing-mounted PMS probes to dust particle sizes. However, as discussed by *J. S. Reid et al.* [2003], some structure can be found by ratioing small and large particle concentrations from the FSSP.

[70] Figure 14 gives particle ratios for four selected flights. Here we use particles in the 1.5–3 μm diameter range from the FSSP as the tracer species since particles in this size range have a mean settling velocity no more than ~25 m per day. We compare particle numbers in the 3–6, 6–11, 11–14, and 14–17 μm diameter ranges to the number in the 1.5–3 μm diameter range and calculate the ratio of small to larger particles. All profiles shared some characteristics. The ratio of small to large particles is a minimum in the marine boundary layer. This is probably due to the presence of large sea salt particles. Conversely, the ratio of small to large particles increases significantly in the uppermost 200 m of the dust layer due to gravitational settling.

[71] For the most part, the FSSP did not detect any change in particle size ratios within the bulk of the dust layers for SAL conditions. For example, particle ratios did not vary systematically with height for the 28 June and 21 July cases by more than ~20%. Over the height range of the entire dust layer for the 20 July case (between 3000 and 5000 m), steeper gradients in particle size ratios are visible. Interestingly, for 20 July, these gradients in size do not follow the layering structure (we would expect an enrichment in large particles below the layers).

[72] An exception to the mostly static size distribution behavior was observed during dust events of 4, 5, and 6 July where a gradient of 40% in particle ratios is found between the top and bottom of the dust layer for all size bins. This can be seen in the 5 July case in Figure 14. All three days of this event exhibited similar behavior. Consider the 6 July case for further examination (Figure 15). Atmospheric thermodynamic soundings along with particle profiles and ratios are shown. On this day a strong SAL was present with a well-defined trade inversion at 1.2 km. Midvisible optical depths were ~0.25. The vertical profile of estimated mass shows no overall trend from the surface to the 2600 m level. A second thick layer is also visible from 2600 m to 5000 m. On the basis of the 1.5–3 μm diameter particle concentration, a more typical SAL vertical distribution is present. However, larger particles (and hence dust particle mass) is more evenly distributed. Comparing the relative amounts of the two particle size ranges with those in Figures 9–12 we can immediately see that smaller particles are strongly enhanced at upper levels. This can be clearly seen in Figure 15c where particle size ratios increase by more than a factor of five with height.

[73] It is important to close this section with a reminder that despite these changes in particle size ratios, we did not find a shift in the area and volume distributions from the FSSP. Indeed, all of the cases shown in this section have nearly identical higher moment distributions as the larger particle counts all covary together due to instrument uncertainties. However, we can clearly see that there are differences in the relationship between particle size distribution and the relative vertical distribution of the dust. This is discussed further in section 5.

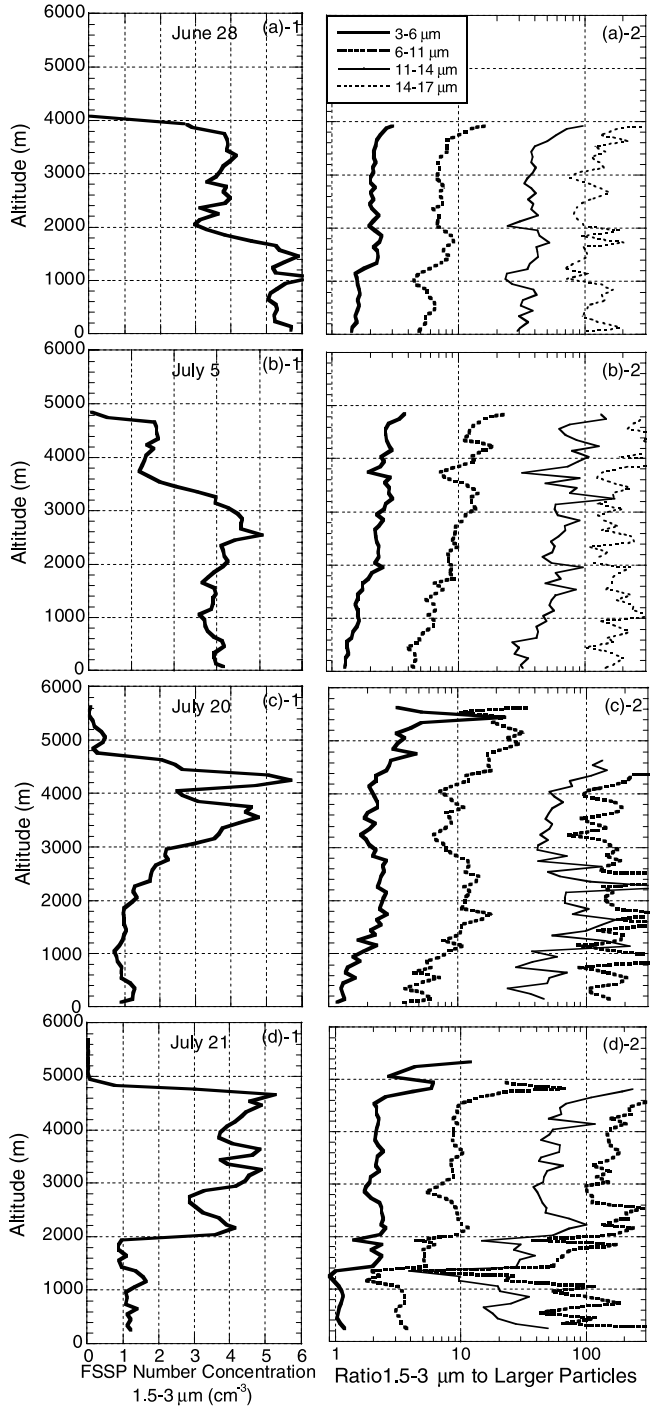

Figure 14. Vertical distributions of particle number and ratios for 28 June and 5, 20, and 21 July 2000. First column, FSSP number concentration in the 1.5–3 μm diameter range. Second column, ratios of the number of particles in the 1.5–3 μm diameter range to the number concentration in the 3–6, 6–11, 11–14, and 14–17 μm diameter range.

4.4. Lidar and Radiosondes

[74] The Navajo data has demonstrated that the vertical distribution of dust mass and size can be at times very

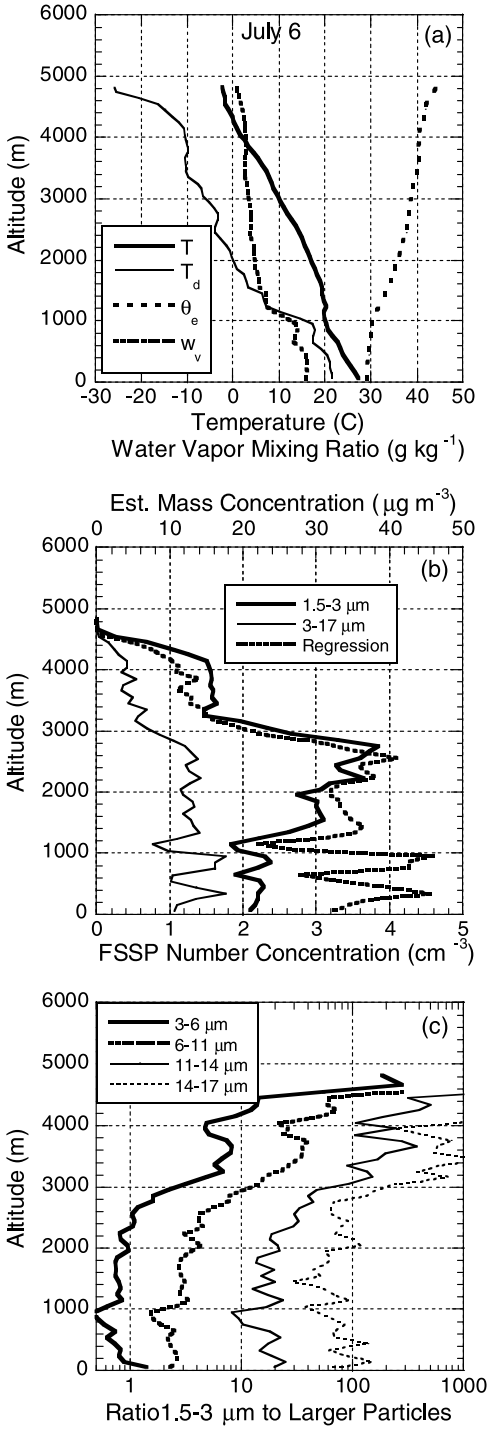

Figure 15. Vertical distribution information for 6 July 2000. (a) Thermodynamic state variables temperature (T, thick solid line), dew point (T_d, thin solid line), equivalent potential temperature (θ_e), and water vapor mixing ratio (ω_v, tight dash line). (b) FSSP number concentration (1.5–3 μm, thick solid line; 3–17 μm, thin solid line), and estimated coarse mode particle concentration (dashed line). (c) Ratios of the number of particles in the 1.5–3 μm diameter range to the number concentration in the 3–6, 6–11, 11–14, and 14–17 μm diameter range.

complex. Since the Navajo collected data for only 61 hours out of the 28 day field campaign it is difficult to extrapolate these findings to the entire study period and determine how the dust's properties relate to the meteorology of the region. This can be done by examining MPLNET lidar data from the Cabras Island site along with atmospheric thermodynamic soundings. Figure 16 presents estimated aerosol particle extinction from the MPL from 28 June 18 UTC to 23 July 0 UTC period. Superimposed on these time series are the estimated trade inversion heights (purple dots) derived from radiosondes released at San Juan Airport, PR. *Livingston et al.* [2003] compared these estimated extinction values to their airborne Sun photometer on the Navajo for four over-flight cases (6, 13, 16, and 21 July). Above 1 km in altitude, they found good agreement. Below 1 km the MPL tended to overestimate extinction by ~25% due to the presence of clouds and the use of a height independent lidar ratio. The FSSP surface area concentrations showed a vertical structure that matched the MPL structure; however, extinction-to-area ratios often differed from layer to layer (individual comparisons with the FSSP are included in the work by *Livingston et al.* [2003]).

[75] Comparison of Figure 16 with the Navajo data in Figures 9–12 shows that qualitatively the MPL captures the vertical distribution of the dust well. In Figure 16 we can clearly see the passing of the significant dust events: 28 June to 6:00 UTC 30 June, 0 UTC 4 July to 0 UTC 7 July, 20 UTC to 8 July to 0 UTC 11 July, 12 UTC 14 July to 20 UTC 16 July, and 10 UTC 20 July to 18 UTC on 22 July (no lidar data were available after this time). From the lidar data these events typically lasted 48 hours, although dust was typically present on most days in some amount [*E. A. Reid et al.*, 2003; Savoie et al., submitted manuscript, 2003a]. Dust maximum altitudes tracked the Navajo data well, with maximum altitudes typically ranging from 3–5 km, with a maximum of 5.5 km on 21 July. The superimposed estimated trade inversion heights from the radiosondes shows the systematic oscillation of the easterly wave influences with a period of ~4 days and maximum inversion heights at 3–5 km. With the advection of a strong SAL, trade inversions dropped to 1–2 km in altitude.

[76] Based on this lidar and radiosonde data, it is clear that the vertical distribution and dynamics of dust is even more complicated than was suggested in the Navajo data. Consider the 21 July event again as what is considered typical "SAL transport." The relatively clean conditions of 19 July gave way to dust and a SAL on 20 July as the trade inversion descended from 2.5 to 1.5 km. Over the next 48 hours, the trade inversion oscillated between ~1.2 and 2 km. Dust in the SAL was not evenly distributed, but showed consistently, like the Navajo data, that dust was transported in coherent sheets. These sheets gradually shift in altitude along with the trade inversion, as the SAL is dynamically forced by the large scale supra-SAL subsidence aloft and conditions near the surface. This tracking between the trade inversion height and dust layers can also be seen in the 15 July case, where despite the presence of dust at lower altitudes a clear SAL dust layer can be seen between 2 and 3 km that is gradually decreasing in altitude along with the trade inversion.

[77] The lidar data also in part confirms the findings that dust can also be dominant below the trade inversion. The

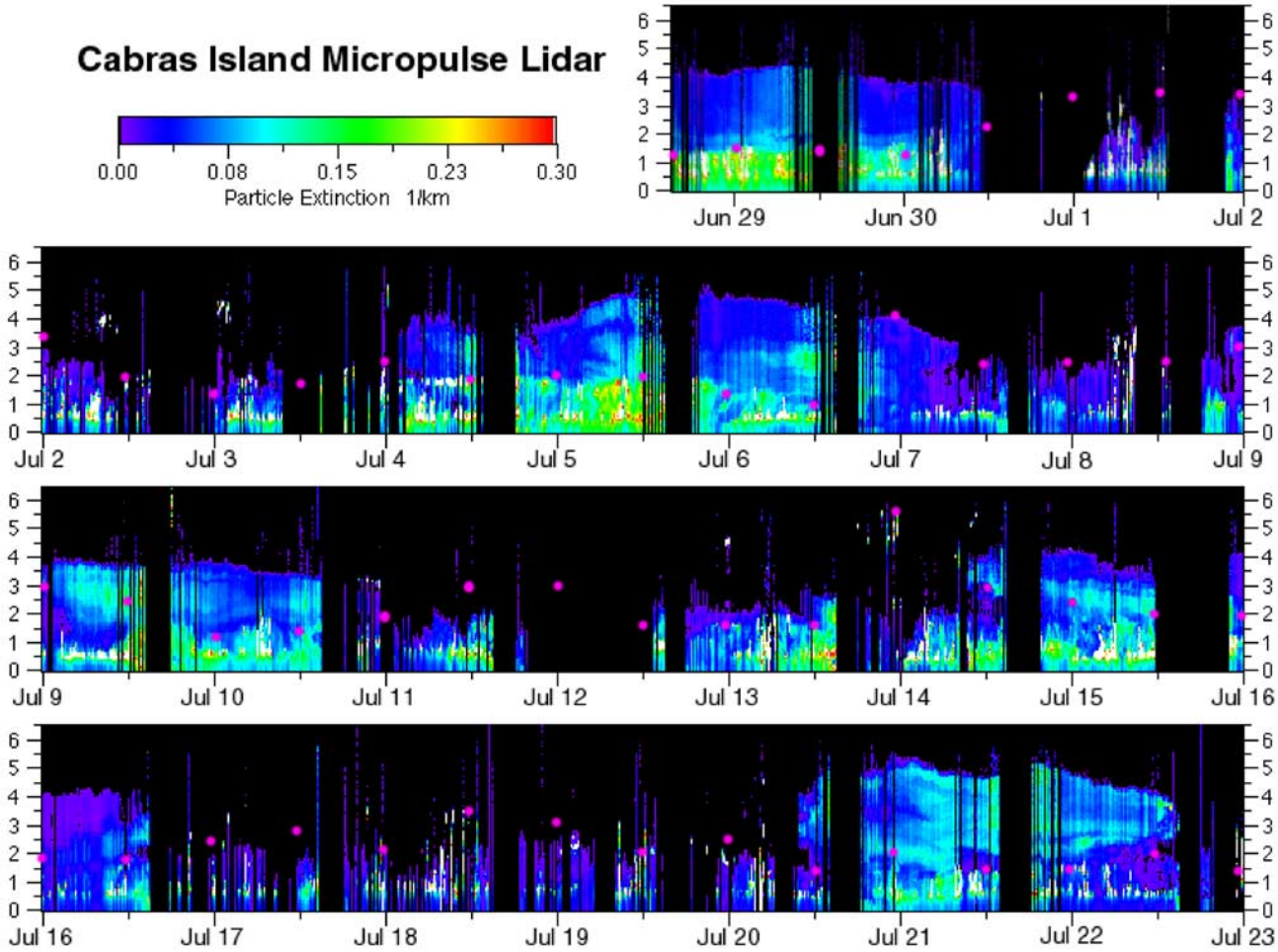

Figure 16. Estimated atmospheric light extinction values from the micropulse lidar station at Cabras Island. Purple dots indicate the estimated trade inversion height from the San Juan Airport radiosonde data.

28–29 June case shows clearly and strongly dust in the MBL and CBL despite the presence of a strong SAL. The days following this event showed few particles above 3 km and surface filter measurements by Savoie et al. (submitted manuscript, 2003a) found that dust was still the dominant aerosol species in the MBL. The Navajo soundings suggested a gradual shift from more low level transport early in the study, to more uniformly distributed dust, to an upper level SAL transport. On the basis of the lidar data we find that upper level SAL dust transport occurred sporadically in earlier periods as well. These elevated layers typically passed quickly from four to eight hours. For example, for 6 July after the Navajo flight the lidar shows a dust layer aloft between 2 and 3 km for ~8 hour period even though the SAL extended as low as 1.1 km. Similarly, the 9 July event was initiated with a dust layer aloft between 2 and 4 km. Lower level transport was also observed later in the study as well. Dust is strongly evident at lower levels late in the day on 13 July (after the flight) and is corroborated at the surface through impactor data [*E. A. Reid et al.*, 2003].

[78] A valuable aspect of coupling MPL data with the radiosondes is to observe the relationship between dust events and the easterly waves. It is often suggested that dust events follow the passage of easterly waves [e.g., *Carlson and Prospero*, 1972; *Westphal et al.*, 1987]. However, after examination of Figure 16 it is unclear if the dust is following, leading or even at times within the easterly wave. With the exception of the very moist cases (e.g., 7 and 14 July) it often appears that the height of the trade inversion is not an indicator as to the vertical distribution of the dust. In the following section, we analyze MPL, radiosonde, Navajo, and AERONET data and gain insight into the relationship between dust properties and the transport meteorology.

5. Analysis and Discussion

[79] The PRIDE campaign monitored six significant dust events (five by lidar) each with its own individual character and typically outside the commonly used conceptual models. Given what is known about the 2000 summer dust season, we first must ask if what we found can be considered "typical." Certainly there were a number of meteorological issues we must concern ourselves with. First, AOTs measured by AERONET Sun photometers on the coast of Africa suggest ~30% (or 1 standard deviation) lower dust

production for 2000 than for other years. This is consistent with the observed more southern track of easterly waves out of Africa and (counterintuitively) drier conditions in the source regions. Easterly wave activity was also further south than what is normal in the Caribbean as well as bringing fairer weather to the Greater/Lesser Antilles. Thus we may have been observing the characteristics of the more northerly half of the dust plume. However, as mean and peak AOTs as well as the temporal patterns of dust in the Caribbean were consistent with other years there is no reason to suspect that what was observed during PRIDE was an anomaly.

[80] The data collected during PRIDE suggests that we may need to reevaluate our conceptual models of long range transport of Saharan dust. Outstanding questions include determining the key factors controlling dust vertical distribution and the relationship between dust and the easterly waves. We can examine these questions by first separating microphysical, local meteorological and long range transport processes. These include dust particle gravitational settling, dry convection and isolated moist convection (i.e., convection not associated with an easterly wave event). Long-range transport processes include dust properties at the coast of Africa and interactions with easterly waves and other synoptic scale phenomena such as large scale differential advection and subsidence. Because the subtropical Atlantic Ocean is in a data void and numerical weather models do not have the resolution to fully model the atmosphere, the relative importance of these mechanisms is uncertain. However, we can examine these processes individually and speculate as to their impact.

[81] Gravitational settling has often been discussed as a first order process for African dust [e.g., *Ellis and Merrill*, 1995]. *Colarco et al.* [2003] has also proposed and supported with some modeling data that settling along with downward transport are causal factors for determining the vertical distribution of dust. However, in the context of the PRIDE field campaign experimental data, we feel Stokes settling likely has little effect on the bulk structure of dust plumes. First, consider that 90% of the mass and light scattering is associated with particles less than 8 μm in aerodynamic diameter [e.g., see *J. S. Reid et al.*, 2003]. At 8 μm, settling velocities are 0.25 cm s^{-1}, or 215 m day^{-1}. Over 6 days of transport, this corresponds to ~1.2 km. For a 5 μm aerodynamic diameter particle (where the mass median diameter likely lies), settling would be ~100 m day^{-1}, or 0.6 km over 6 days. Considering that the SAL dust layers were typically ~2–3 km thick, gravitational settling could not account for the overwhelming shift of dust from the SAL to the MBL and CBL. This is further demonstrated in the PCASP data in Figure 11 where particles in the 0.3–1.1 μm range (which should have settling rates less than 6 m day^{-1}) are also seen above and below the trade inversion.

[82] Although gravitational settling does not account for the large-scale shifts in dust vertical distribution, it still can give insight into the transport process. On the basis of calculations above, we would expect to see a great deal of depletion of large particles at the top of SAL layer. However our findings in Figure 14 show depletion only in the uppermost 300 m, not on the order of a kilometer. This would be particularly evident in Figure 14c with the presence of strong shallow layering. Certainly, part of this is due to insensitivities of dust size to the FSSP instrument, but we would expect more change than this. Although not in numbers to significantly skew a size distributions, studies such as *Betzer et al.* [1988] and *E. A. Reid et al.* [2003] have found dust particles larger than 20 μm in Hawaii and Puerto Rico, respectively. A 20 μm particle should settle at velocities greater than 1 cm s^{-1}, or 1 km per day. Recently, *Maring et al.* [2003] found that after comparing dust aerodynamic particle sizer data in Izaña Tenerefe, Canary Islands with data from the Cabras Island site during PRIDE that there did not appear to be any change in dust particle size distribution for particles less than 8 μm in geometric diameter. Finally, there is also the 5–6 July dust event where we did find a significant gradient in dust size throughout the dust layer. Why is a gradient found on this day but no others? These issues suggest that there are other processes that appear to keep dust particles aloft.

[83] Another possibility to explain the variance in dust vertical profiles is that local dry or moist convection may be playing a role. If present, such convection would mix the atmosphere and reduce any particle size gradients. However, convective processes are isolated to specific portions of the atmosphere. By definition, the SAL is neutrally stable without convection. This lack of convective activity is demonstrated by the presence of thin dust layers that span hundreds of kilometers. In Figure 16 we can see that these layers can exist for 12 hours or more. If significant, convection would quickly dissipate any such layering. Hence it is likely that dry convection is only active in the MBL (i.e., altitudes <500 m). On the other hand, moist convection in the CBL has a more significant role in dust exchange between the SAL and MBL. For the most part, isolated clouds are not mixing dust from deep within the SAL to the surface. Isolated clouds were often observed penetrating the trade inversion by as much as a kilometer on days with a strong trade inversion, but these clouds were rare. Further, such mixing would be evident with increased water vapor mixing ratios inside the SAL. On most days however, moist convection and entrainment have a strong role to play in the exchange of dust from the trade inversion to the MBL. If dust passes through the trade inversion into the CBL, clouds would mix the dust and transport it into the MBL much more rapidly than gravitational settling. With roughly 20–50% convective cloud cover in the CBL on most days, this process cannot be ignored. On days where there was increased convection with a trade inversion that is weak (or at high altitudes) such as on 2–4, 9, and 14 July, this is likely a significant process.

[84] We must consider, however, that in the first third of the study period dust was more uniformly distributed in the atmosphere despite the presence of a strong SAL (e.g., 28–29 June and 5–6 July events). In many cases, the concentration of the dust did not vary at all across the trade inversion. On these days, could moist convection be a causal factor? Since there was a strong trade inversion on these days, clouds were not penetrating into the SAL. Hence dust must be transported across the trade inversion by some mechanism before moist convection can act. As discussed above, gravitational settling would allow larger particles to cross the trade inversion but cannot entirely account for such a dramatic shift in vertical distribution.

[85] Another possible mechanism is that the trade inversion is evolving along with the SAL during transport. *Albrecht* [1979] showed that the height of the trade inversion is dependant on regional effects such as sea surface temperature, surface wind speed, and radiative heating. In addition, the SAL can be acted on by upper level subsidence. We must then recognize that dust in the SAL and the trade inversion are somewhat decoupled. Consider the 21 July case where the dust lower boundary is 300 m above the trade inversion. In this case, the trade inversion may have lowered and strengthened over the previous 24 to 48 hours. We can see from Figure 16 that when this occurred, dust layers follow the trade inversion to lower levels. Conversely, for the more uniformly distributed dust cases, the trade inversion may have increased in height with time and/or weakened. This increase in the inversion height would thus entrain dust from above into the CBL and smooth the dust vertical distribution.

[86] These localized mechanisms probably occur but like previous explanations cannot explain those circumstances when dust is dominant at lower levels either, (such as the 28–29 June and 3 July event). A feasible hypothesis is that dust vertical profiles are influenced by in altitude during transport coupled with differential advection. Certainly in a receptor sight as far away from the source region as Puerto Rico, the vertical profile of dust is dictated by the separate transport of many individual layers. Large scale shifts in dust vertical profile can occur through interactions of dust laden air with easterly waves or, as hypothesized by *Colarco et al.* [2003] through large scale subsidence. As discussed by *Carlson and Prospero* [1972] and *Karyampudi et al.* [1999], large dust events seem to follow easterly waves. However, the speed of easterly waves can vary relative to the mean flow. Hence some dust-laden air should pass through the influence of easterly waves before they reach the western Atlantic Ocean. In the case of PRIDE, where the more moist portions of the easterly waves propagated south of Puerto Rico, it is possible that deep non-precipitating convection will cause the atmosphere and dust to mix without significant scavenging. If such mixing were to occur, water vapor would be mixed as well as the dust. Hence any case where we find a strong SAL with water vapor mixing ratios on the order of 5 g kg^{-1} (e.g., 28 June and 6, 10, 15, 21 July) excludes the possibility that it passed through an active portion of an easterly wave. However, it is possible for areas below the trade inversion to be transported from the southeast where such mixing could occur in the easterly waves, and then have a dry SAL layer advected into the region aloft from the northeast.

[87] Similarly shifts in altitude can also be explained by large-scale subsidence in the region [*Colarco et al.*, 2003]. *Colarco et al.* [2003] showed that for the 5, 10, and 15 July events at Puerto Rico could be modeled to be at lower altitudes due to this process. Because such a process would act on the SAL as a whole, we feel it cannot explain on its own the sheer depth of the dust layers. Besides, large-scale subsidence cannot force dust into the MBL without entrainment by dry or moist processes. However, if a shift in dust altitude were coupled by differential advection (e.g., lower level dust passed through a region of increased subsidence and more entrainment than the upper air mass), such a mechanism becomes much more plausible.

[88] We can test these hypotheses by examining a back trajectory analysis. Figure 17 presents back trajectories for two levels for the dust maximums of 28 June and 5, 9, 15, and 21 July from the NOAA Realtime Environmental Applications System Hybrid Single-Particle Lagrangian Integrated Trajectory (HYSPLIT4 Model, see http://www.arl.noaa.gov/ready/hysplit4.html, NOAA Air Resources Laboratory, Silver Spring, Maryland) system. Back trajectories were run for the 300 and 3000 m start altitudes at Puerto Rico for 144 hours. Because these trajectories are made in an area of a data void, they are probably only reliable for 3 days (for example the 21 July case does not even have the trajectories leaving Africa). Even so, the trajectories indicated that in the first half of the study when dust was more dominant in the MBL and CBL, upper air masses in the SAL were more likely to have a southerly component. Conversely, MBL air masses had a more northerly component. It is in these more northern regions of the subtropics where we would expect more large-scale subsidence. However, altitude plots do not entirely support this. Descending air masses are clearly visible for the 28 June and 15 and 21 July cases. However, the 5 and 9 July trajectories are relatively constant in altitude. Since both lower level and SAL transport was seen in both of these regimes, the altitude trajectory plots are inconclusive.

[89] It is noteworthy that in the later half of the study (after 10 July) when dust become more prevalent aloft upper and lower air masses tended stay along the same geographic tract for several days. Hence it plausible that days with more uniform vertical profile may in part be due to the combination of separate air masses from different regions. Even so, we must recognize that when upper and lower trajectories track that they are advected at different speeds. Hence the low level dust events on 10, 13, and 16 July may be lagging the dust event aloft which arrived on 9 and 15 July.

[90] Finally, we can revisit the possibility that the vertical distribution of dust was predefined as it passes from Africa to the Atlantic Ocean as was originally hypothesized by *Reid et al.* [2002]. It is commonly assumed that dust is transported to sea in elevated SAL layers in the strong easterly trade winds as strong westerly monsoonal flow forms near the coast and blows inland. *Chiapello et al.* [1995] suggested that in the winter months, when this flow is weak or nonexistent, dust can be transported to sea in easterly trade winds at the surface. *Reid et al.* [2002] argued that based on the soundings at Dakar, monsoonal flow probably did not develop until later than 5–10 July. Hence it is possible that much of the dust for the 28–29 June or even the 5–6 July case had in fact left Africa with a similar vertical distribution (i.e., dust in the MBL and CBL). A more thorough analysis of NAAPS data suggests that dust vertical distributions did vary on the coast of Africa) (Westphal et al., manuscript in preparation, 2003; http://www.nrlmry.navy.mil/aerosol). The lowest dust altitudes leaving Africa were from storms which formed the 28 June event (950–700 mb). Subsequent events gradually increased in height to a maximum for the storm that caused the 21 July event (800–600 mb). Qualitatively, this matches our findings in Puerto Rico. However NAAPS showed the shift in altitude was somewhat smooth and did not have the more erratic character as

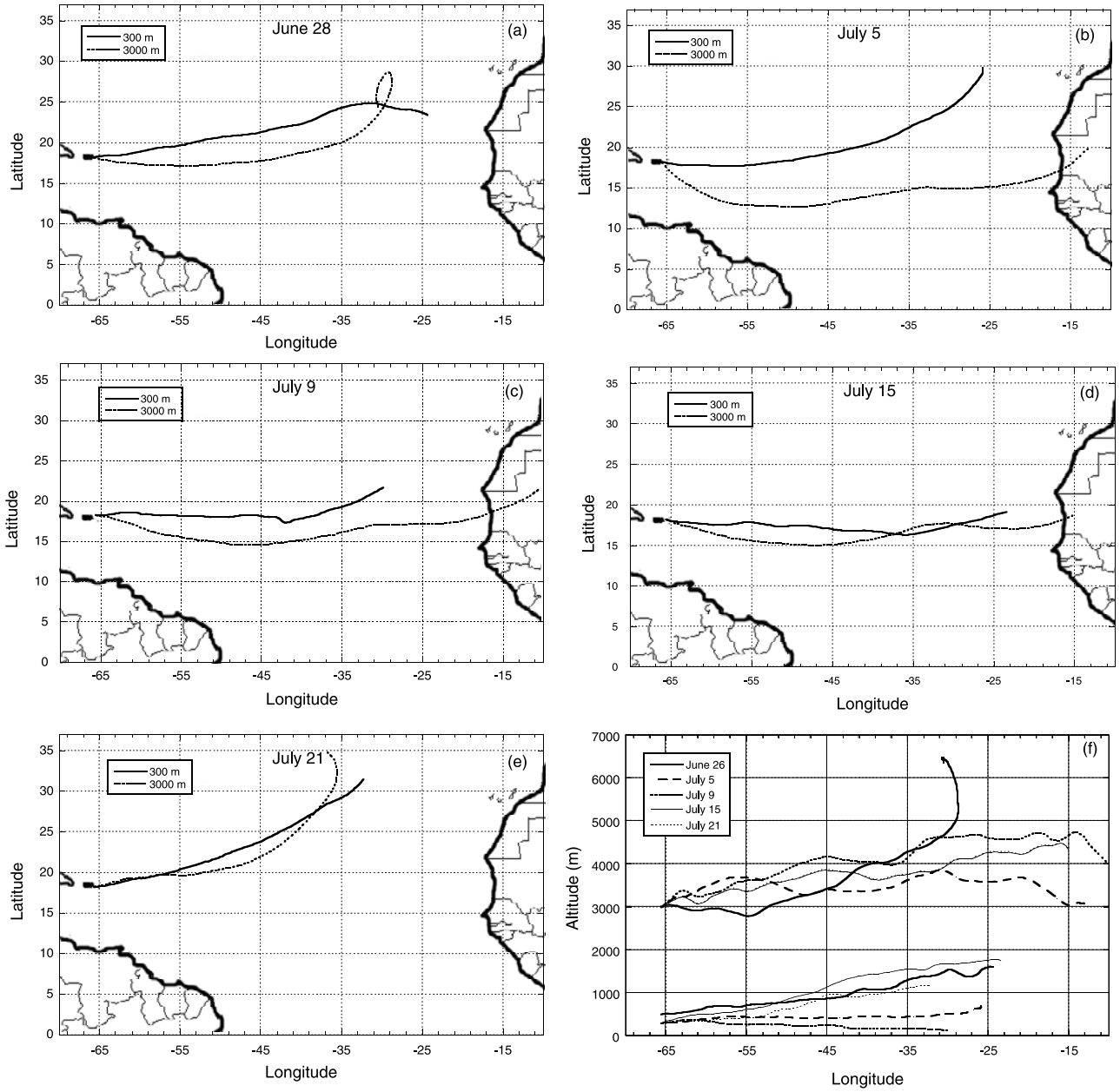

Figure 17. The 300 and 3000 m READY/HYSPLIT 144 hour back trajectories from Roosevelt Roads, Puerto Rico. (a) 28 June 14:00 UTC start time, (b) 5 July 14:00 UTC start time, (c) 9 July, (d) 15 July, (e) 21 July, and (f) altitude plots for Figures 17a through 17e.

seen in Puerto Rico. This behavior is better explained by the differential advection hypothesis.

6. Implications to Conceptual Models

[91] The findings of the PRIDE project cannot be easily generalized to fit any particular conceptual model. It is likely that to some extent, all of the mechanisms discussed in section 5. play varying roles in determining the dust vertical distribution on an event by event basis. However, we can use this data set to scrutinize preexisting conceptual models. In particular, the models of ''Upper level SAL transport'' [e.g., *Karyampudi and Carlson*, 1988; *Karyampudi et al.*, 1999; *Westphal et al.*, 1987] and lower level/uniform transport [e.g., *Chiapello et al.*, 1995; *Formenti et al.*, 2001; *Reid et al.*, 2002] warrant further examination.

[92] *Karyampudi et al.* [1988] describes the SAL conceptual model as forming as a result of large dust storms which are mixed up to 5 to 6 km over Africa due to intense solar heating. These dust events are between two consecutive easterly wave troughs. As the dust is advected to the west African coast by easterly trade winds, it is undercut by westerlies in the MBL forming a well-mixed dust layer aloft. As the transport continues westward, the top of the SAL diminishes in altitude slowly due to large scale subsidence aloft. Maximum dust concentrations remain highest in the ridge between the two easterly waves. *Karyampudi et al.* [1999] (hereafter referred to as K99)

reexamined this model by analyzing a September 1994 dust outbreak using Lidar-in Space Technology Experiment (LITE) data coupled with ECMWF meteorology and Meteosat optical depths. Among their conclusions were the following. (1) There was constant dust advection off Africa in association with the Harmattan haze punctuated by fresh high AOT dust outbreaks instead of simply individual dust events. (2) The top of the dust layer over the Atlantic descended rapidly. They suggest this is due to the fallout of giant particles. (3) High dust concentrations near the southern edge of the SAL can extend downward into the MBL. They suggest this may be a consequence of sedimentation and vertical mixing due to strong vertical wind shears associated with the midlevel jet. (4) The MBL under the SAL appears to be saturated with aerosol particles. They suggest this is due to residual dust particles and sea salt. (5) The trade wind inversion was well defined in the LITE data in the northern edge of the plume. However, in the center of the plume the trade inversion was not visible due to high dust concentrations and optical depths.

[93] The findings of the PRIDE campaign support the observational evidence presented by K99, but differ somewhat in interpretation. Let us consider these points individually. First, the findings from the AERONET Sun photometers in Dakar and Cape Verde verify the K99 finding that there is continuous dust advection off of the coast of Africa in September 1994. For the year 2000, this feature also occurred in the summer months (mid-May to mid-October). There is less agreement with their second point that the top of the dust layer is descending rapidly due to gravitational settling. On the basis of our findings, much of the lidar backscatter is due to particles with aerodynamic diameters less than 5 μm which do not have an appreciable settling velocity.

[94] The final three points listed above from K99 are related to dust vertical distribution. Clearly, the LITE data shows that dust can in fact be significant in the MBL well into the summer transport season. However, K99 interprets this feature as secondary to the principal dust transport. As we have shown dust can in fact have higher concentrations in the MBL than the SAL and cannot easily be dismissed as ''residual''. Similarly, we have shown that the trade inversion is frequently decoupled from the SAL. Hence the appearance of a strong gradient in dust is not necessarily indicative of the strength or height of the trade inversion. As K99 pointed out, the lidar data are difficult to interpret due to the presence of hydrated sea salt near the MBL inversion. This can be seen in the work by *Livingston et al.* [2003] and our own Figure 16, the increased relative backscattering to extinction ratio due to large sea salt particles can quickly dampen the dust signal. So even here it is not clear if K99 is seeing salt/cloud artifact in the MBL or dust.

[95] Finally, K99's finding that dust was found at lower levels in the southern half of the dust plume while more typical ''SAL transport'' still occurred to the north would indeed suggest vertical mixing and demonstrate the complicated nature of dust transport. Further, such a finding does not necessarily exclude the possibility that the dust left the African coast with that particular north-south gradient in vertical distribution.

[96] In contrast to the *Karyampudi et al.* [1988] conceptual model, *Chiapello et al.* [1995] suggested a wintertime low level dust transport mechanism for those occasions when westerly onshore flow was not present. Consequently, there was no MBL for the SAL to slide over and dust would be transported off Africa at lower levels. *Reid et al.* [2002] suggested that this mechanism may extend through the spring. The meteorological data presented by *Chiapello et al.* [1995] and *Reid et al.* [2002] clearly show that this onshore flow component can weaken thus allowing low level transport. Further, such flow is much more likely to form in the winter months. However, in the context of the PRIDE field campaign conducted in the early summer, what percentage is due to low level transport and what fraction, if any, is due to other mixing phenomena? How does this relate to K99's findings of a north-south gradient in vertical distribution? Additional evidence is given by *Formenti et al.* [2001], where both low-level and more ''SAL-ish'' transport was observed within just days of one another in South America. This suggests that both the vertical distribution of dust at Africa and vertical mixing through moist convection are likely equally important over long periods of time. The PRIDE data shows a gradual change in dust vertical distribution, most likely due to the gradual development of onshore monsoonal flow. However, such flow is unlikely to change over the course of 2 to 3 days as would be required to explain *Formenti et al.*'s [2001] results.

[97] Any further development on conceptual models requires an extensive analysis of the relationship between dust transport and the easterly tropical waves. Clearly, convergence and convection ahead of the wave axis should impact dust vertical distribution. Perhaps an analysis could include a simple comparison of dust vertical distribution with easterly wave strength and relative wave and flow speeds. If the wave and flow speed are equal, the SAL would be ''book ended'' and any SAL character should be preserved. If the wave speed is greater than the flow (as is not uncommon over Africa and the East Atlantic), yields convection westward (ahead) of the wave axis. Conversely, periods when the flow-passes through the wave would result in convergence and convection behind the wave. A prolonged study of dust vertical distribution (say through ground and space-borne lidar) coupled with such a meteorological analysis is clearly necessary.

[98] Regardless of the mechanisms, it is clear that the issues surrounding dust vertical distribution and transport are complicated. Reexamination of other studies yields supporting evidence that lower level transport may be more common than originally thought. As discussed above, K99 and other studies corroborate our findings. However these corroborating studies, like PRIDE, are limited in temporal and spatial scope. Much longer term studies using ground and satellite based remote sensing data are required. Until lidar data are more prevalent, more crude methods must be applied to determine the vertical distribution of dust over long periods of time. One opportunity is from colocated Sun photometer and surface filter measurements. *Smirnov et al.* [2000b] found at Barbados that when averaged over several weeks, surface dust concentrations were highly correlated with dust AOT. However, on a daily basis this correlation reduces significantly indicating that variability in dust vertical distribution is a more common occurrence. A more complete

analysis is given by Savoie et al. (submitted manuscript, 2003a).

7. Summary and Conclusions

[99] This paper gave an overview of the Puerto Rico dust Experiment (PRIDE) field campaign, and in particular focuses on the atmospheric properties of the Caribbean region and dust vertical distribution. This is done by examination of surface-based AERONET Sun photometer and micro-pulse lidar data, and airborne data collected on a twin engine Piper Navajo.

[100] At Puerto Rico for PRIDE, six significant dust events reached the island on 28–29 June, 4–6 July, 9–10 July, 15–16 July, 21 July, and 23 July. Midvisible aerosol optical thickness (AOT) at Puerto Rico varied from clean marine conditions (0.07) to high dust loading periods (AOT > 0.5). The average midvisible AOT was 0.24. In comparison AOTs at the coast of Africa had a higher mean value ($\sim$0.45) with peak events up to 0.8. These optical depths are somewhat lower than the previous 3 years, and may be related to a Caribbean-wide negative precipitation anomaly.

[101] The vertical distribution of dust in the Caribbean was found to be highly variable during the PRIDE field campaign, with both "typical Saharan Air Layer (SAL)" and lower level transport of dust being observed. Dust frequently reached altitudes of 5 km. The presence of dust in the marine boundary layer was not correlated with any "typical" atmospheric sounding profile, in particular it did not correlate with the strength of the trade inversion in the Caribbean. In fact, as the trade inversion is heavily influenced by local conditions, the SAL and trade inversions can be decoupled.

[102] The transition between lower level and upper level dust transport occurred slowly with sporadic deviations over the course of the field study. However, embedded within individual events were well defined layers above the trade inversion. These layers could persist for several hundred kilometers in both the along and cross flow directions.

[103] For the most part, we did not find strong gradients in dust particle size with height, except in the uppermost 300 m of the dust. This finding including cases with very strong layering. The exception to this behavior was during 4–6 July 2000 where strong particle size gradients were observed from the trade inversion up to the maximum dust altitude of 5 km.

[104] We analyzed our data and tried to determine the causal factors dictating the vertical distribution of dust. In most circumstances, gravitational settling does not appear to be an important process in dictating dust vertical distribution. We conclude that to a large degree that the dust's vertical distribution as it leaves Africa (i.e., dust is transported across the Atlantic ocean with its vertical character already defined) is the only reasonable explanation as to why dust concentrations can be a maximum in the marine boundary layer such as the June 28 case. However, shifts in dust mean altitude (due to the combined effects of large scale subsidence such as hypothesized by *Colarco et al.* [2003] and vertical mixing due to moist convection) coupled with differential advection is a likely mechanisms to cause the chaotic nature of the dust vertical distribution for the rest of the study.

[105] We further analyzed our findings in the context of established conceptual models of dust transport. We scrutinized *Karyampudi and Carlson* [1988] and the updated findings of *Karyampudi et al.* [1999]. During the PRIDE campaign, we found many of the same discrepancies in the work by *Karyampudi and Carlson* [1988], as did *Karayampudi et al.* [1999] using a combination of lidar, satellite, and meteorological data. However, we differ in some of the interpretations of the results. Most importantly, *Karyampudi et al.* [1999] did find evidence of dust in the MBL but concluded that it was "residual" to the main transport (which we dispute).

[106] **Acknowledgments.** We are grateful to the personnel at Naval Station Roosevelt Roads, including ENS Roger Hahn and the entire staff at North Atlantic Meteorology and Oceanography Detachment, Roosevelt Roads for all of their support during the field deployment. We also would like to thank the whole Gibbs Flite Center crew, including William "Buzz" Gibbs, Michael Kane, Michael Hubble, and Lyle Richards. Additional thanks for Navajo support are due to Duane Allen, NASA Ames Research Center. We appreciate comments from Richard Paulus, SSC-SD. PRIDE funding was provided by the Office of Naval Research Code 322, including N0001401WX20194, and the NASA Mission to Planet Earth program office. NCEP reanalysis data and images were provided by the NOAA-CIRES Climate Diagnostics Center, Boulder, CO from their Web site at http://www.cdc.noaa.gov. Precipitation data were provided by NOAA/NWS NCEP Climate Prediction Center, Camp Springs, MD from their web site at http://www.cpc.ncep.noaa.gov.

References

Albrecht, B. A., A model of the thermodynamic structure of the trade-wind boundary layer: Part II Applications, *J. Atmos. Sci.*, *36*, 90–98, 1979.

Augstein, E., H. Schmidt, and F. Ostapoff, The vertical structure of the atmospheric planetary boundary layer in undisturbed trade winds over the Atlantic Ocean, *Boundary Layer Meteorol.*, *6*, 129–150, 1974.

Betzer, P. R., et al., Long-range transport of giant mineral aerosol particles, *Nature*, *336*, 569–571, 1988.

Campbell, J. R., D. L. Hlavka, E. J. Welton, C. J. Flynn, D. D. Turner, J. D. Spinhirne, V. S. Scott, and I. H. Hwang, Full-time, Eye-safe cloud and aerosol lidar observation at Atmospheric Radiation Measurement Program Sites: Instrument and data processing, *J. Atmos. Oceanic Technol.*, *19*, 431–442, 2002.

Carlson, T. N., and J. M. Prospero, The large-scale movement of Saharan air outbreaks over the northern equatorial Atlantic, *J. Appl. Meteorol.*, *11*, 283–297, 1972.

Chiapello, I., G. Bergametti, F. Dulac, L. Gomes, B. Chatenet, J. Pimenta, and E. S. Suares, An additional low layer transport of Sahelian and Saharan dust over the north-eastern tropical Atlantic, *Geophys. Res. Lett.*, *22*, 3174–3191, 1995.

Claquin, T., M. Schulz, Y. Balkanski, and O. Boucher, Uncertainties in assessing radiative forcing by mineral dust, *Tellus, Ser. B*, *50*, 491–505, 1998.

Colarco, P., et al., Saharan dust transport to the Caribbean during PRIDE: 2. Transport, vertical profiles, and deposition in simulations of in situ and remote sensing observations, *J. Geophys. Res.*, *108*(D19), 8590, doi:10.1029/2002JD002659, in press, 2003.

Collins, D. R., et al., In situ aerosol-size distributions and clear-column radiative closure during ACE-2, *Tellus, Ser.B.*, *52*, 498–525, 2000.

Delany, A. C., D. W. Parkin, J. J. Griffin, E. D. Goldberg, and B. E. F. Reinman, Airborne dust collected at Barbados, *Geochim. Cosmochim. Acta*, *31*, 885–909, 1967.

Duce, R. A., et al., The atmospheric input of trace species to the world ocean, *Global Biogeochem. Cycles*, *5*, 193–260, 1991.

Ellis, W. G., and J. T. Merrill, Trajectories for Saharan dust transport to Barbados using Stoke's law to describe gravitational settling, *J. Appl. Meteorol.*, *34*, 1716–1726, 1995.

Formenti, P., M. O. Andreae, L. Lange, G. Roberts, J. Cafmeyer, I. Rajta, W. Maenhaut, B. N. Holben, P. Artaxo, and J. Lelieveld, Saharan dust in Brazil and Suriname during the Large-Scale Biosphere-Atmosphere Experiment in Amazonia (LBA)-Cooperative LBA Airborne Regional Experiment (CLAIRE) in March 1998, *J. Geophys. Res.*, *106*, 14,919–14,934, 2001.

Fyfe, J. C., Climate simulations of African easterly waves, *J. Clim.*, *12*, 1747–1769, 1999.

Ganor, E., and Y. Mamane, Transport of Saharan dust across the eastern Mediterranean, *Atmos. Environ.*, *16*, 581–587, 1982.

Gao, Y., Y. J. Kaufman, D. Tanre, D. Kolber, and P. G. Falkowski, Seasonal distributions of aeolian iron fluxes to the global ocean, *Geophys. Res. Lett.*, *29*, 29–32, 2001.

Giannini, A., Y. Kushnir, and M. A. Cane, Interannual variability of Caribbean rainfall, ENSO, and the Atlantic Ocean, *J. Clim.*, *13*, 297–311, 2000.

Grist, J. P., Easterly waves over Africa. part I: The seasonal cycle and contrasts between wet and dry years, *Mon. Weather Rev.*, *130*, 197–211, 2002.

Grist, J. P., S. E. Nicholson, and A. I. Barcilon, Easterly waves over Africa. part II: Observed and modeled contrasts between wet and dry years, *Mon. Weather Rev.*, *130*, 212–225, 2002.

Holben, B. N., et al., An emerging ground-based aerosol climatology: Aerosol optical depth from AERONET, *J. Geophys. Res.*, *106*, 12,067–12,097, 2001.

Janowiak, J. E., and P. Xie, CAMS_OPI: A global Satellite-rain gauge merged product for real-time precipitation monitoring applications, *J. Clim.*, *12*, 3335–3342, 1999.

Kalnay, E., et al., The NCEP/NCAR Reanalysis 40-year project, *Bull. Am. Meteorol. Soc.*, *77*, 437–471, 1996.

Karyampudi, V. M., and T. N. Carlson, Analysis and numerical simulations of the Saharan Air Layer and its effects on easterly wave disturbances, *J. Atmos. Sci.*, *45*, 3102–3136, 1988.

Karyampudi, V. M., et al., Validation of the Saharan dust plume conceptual model using lidar, Meteosat, and ECMWF data, *Bull. Am. Meteorol. Soc.*, *80*, 1045–1075, 1999.

Livingston, J. M., et al., Airborne Sun photometer measurements of aerosol optical depth and columnar water vapor during the Puerto Rico Dust Experiment and comparison with land, aircraft, and satellite measurements, *J. Geophys. Res.*, *108*(D19), 8588, doi:10.1029/2002JD02520, 2003.

Maring, H., D. L. Savoie, M. A. Izaguirre, L. Custals, and J. S. Reid, Mineral dust aerosol size distribution change during atmospheric transport, *J. Geophys. Res.*, *108*(D19), 8592, doi:10.1029/2002JD002536, 2003.

Matsumoto, T., P. B. Russell, C. Mina, W. Van Ark, and V. Banta, Airborne tracking Sunphotometer, *J. Atmos. Oceanic Technol.*, *4*, 336–339, 1987.

May, D. A., L. L. Stowe, J. D. Hawkins, and E. P. McClain, A correction for Saharan dust effects on satellite sea surface temperature measurements, *J. Geophys. Res.*, *94*, 3611–3617, 1992.

Moulin, C., H. R. Gordon, R. M. Chomko, V. F. Banzon, and R. H. Evans, Atmospheric correction of ocean color imagery through thick layers of Saharan dust, *Geophys. Res. Lett.*, *28*, 5–8, 2001.

Myhre, G., and F. Stordal, Global sensitivity experiments of the radiative forcing due to mineral aerosols, *J. Geophys. Res.*, *106*, 18,193–18,204, 2001.

Perry, K. D., T. A. Cahill, R. A. Eldred, D. D. Dutcher, and T. E. Gill, Long-range transport of North African dust to the eastern United States, *J. Geophys. Res.*, *102*, 11,225–11,238, 1997.

Prospero, J. M., Long-term measurements of the transport of African mineral dust to the southeastern United States: Implications for regional air quality, *J. Geophys. Res.*, *104*, 15,917–15,927, 1999.

Prospero, J. M., and T. N. Carlson, Vertical and areal distribution of Saharan dust over the western equatorial North Atlantic Ocean, *J. Geophys. Res.*, *77*, 5255–5265, 1972.

Prospero, J. M., R. A. Glaccum, and R. T. Nees, Atmospheric transport of soil dust from Africa to South America, *Nature*, *289*, 570–572, 1981.

Reid, E. A., J. S. Reid, M. M. Meyer, M. Dunlop, S. S. Cliff, A. Broumas, K. D. Perry, and H. Maring, Characterization of African dust transported to Puerto Rico by individual particle and size segregated bulk analysis, *J. Geophys. Res.*, *108*(D19), 8591, doi:10.1029/2002JD002935, in press, 2003.

Reid, J. S., D. L. Westphal, J. M. Livingston, D. L. Savoie, H. B. Maring, H. H. Jonsson, D. P. Eleuterio, J. E. Kinney, and E. A. Reid, Dust vertical distribution in the Caribbean during the Puerto Rico Dust Experiment, *Geophys. Res. Lett.*, *29*(7), 1151, doi:10.1029/2001GL014092, 2002.

Reid, J. S., et al., Comparison of size and morphological measurements of coarse mode dust particles from Africa, *J. Geophys. Res.*, *108*(D19), 8593, doi:10.1029/2002JD002485, in press, 2003.

Reynolds, R. W., and T. M. Smith, Improved global sea surface temperature analysis using optimum interpolation, *J. Clim.*, *7*, 929–948, 1994.

Smirnov, A., B. N. Holben, T. F. Eck, O. Dubovik, and I. Slutsker, Cloud screening and quality control algorithms for the AERONET data base, *Remote Sens. Environ.*, *73*, 337–349, 2000a.

Smirnov, A., B. N. Holben, D. Savoie, J. M. Prospero, Y. J. Kaufman, D. Tanre, T. F. Eck, and I. Slutsker, Relationship between column aerosol optical thickness and in situ ground based dust concentrations over Barbados, *Geophys. Res. Lett.*, *27*, 1643–1646, 2000b.

Smirnov, A., B. N. Holben, Y. J. Kaufman, O. Dubovik, T. F. Eck, I. Slutsker, C. Pietras, and R. Halthore, Optical properties of atmospheric aerosol in maritime environments, *J. Atmos. Sci.*, *59*, 501–523, 2002.

Sokolik, I. N., D. M. Winker, G. Bergametti, D. A. Gillette, G. Carmichael, Y. J. Kaufman, L. Gomes, L. Schuetz, and J. E. Penner, Introduction to special section: Outstanding problems in quantifying the radiative impacts of mineral dust, *J. Geophys. Res.*, *106*, 18,015–18,028, 2001.

Spinhirne, J. D., J. Rall, and V. S. Scott, Compact eye-safe lidar systems, *Rev. Laser Eng.*, *23*, 26–32, 1995.

Swap, R., M. Garstang, S. Greco, R. Talbot, and P. Kallberg, Saharan dust in the Amazon Basin, *Tellus, Ser. B*, *144*, 133–149, 1992.

Swap, R., M. Garstang, S. A. Macko, P. D. Tyson, W. Maenhaut, P. Artaxo, P. Kallberg, and R. Talbot, The long-range transport of southern African aerosols to the tropical South Atlantic, *J. Geophys. Res.*, *101*, 23,777–23,791, 1996a.

Swap, R., S. Ulanski, M. Cobbett, and M. Garstang, Temporal and spatial characteristics of Saharan dust outbreaks, *J. Geophys. Res.*, *101*, 4205–4220, 1996b.

Talbot, R. W., M. O. Andreae, H. Berresheim, P. Artaxo, M. Garstang, R. C. Harriss, K. M. Beecher, and S. M. Li, Aerosol chemistry during the wet season in central Amazonia: The influence of long-range transport, *J. Geophys. Res.*, *95*, 16,955–16,969, 1990.

Tanré, D., Y. J. Kaufman, B. N. Holben, B. Chatenet, A. Karnieli, F. Lavenu, L. Blarel, O. Dubovik, L. A. Remer, and A. Smirnov, Climatology of dust aerosol size distribution and optical properties derived from remotely sensed data in the solar spectrum, *J. Geophys. Res.*, *106*, 18,205–18,219, 2001.

Tegen, I., and I. Fung, The influence on climate forcing of mineral aerosols from disturbed soils, *Nature*, *380*, 419–422, 1996.

Welton, E. J., and J. R. Campbell, Micropulse lidar signals: Uncertainty analysis, *J. Atmos. Oceanic Technol.*, *19*(12), 2089–2094, 2002.

Welton, E. J., J. R. Campbell, J. D. Spinhirne, and V. S. Scott, Global monitoring of clouds and aerosols using a network of micro-pulse lidar systems, in *Lidar Remote Sensing for Industry and Environmental Monitoring*, edited by U. N. Singh, T. Itabe, N. Sugimoto, *Proc. SPIE Int. Soc. Opt. Eng.*, *4153*, 151–158, 2001.

Welton, E. J., K. J. Voss, P. K. Quinn, P. J. Flatau, K. Markowicz, J. R. Campbell, J. D. Spinhirne, H. R. Gordon, and J. E. Johnson, Measurements of aerosol vertical profiles and optical properties during INDOEX 1999 using micropulse lidars, *J. Geophys. Res.*, *107*(D19), 8019, doi:10.1029/2000JD000038, 2002.

Westphal, D. L., O. B. Toon, and T. N. Carlson, A two-dimensional numerical investigation of the dynamics and microphysics of Saharan dust storms, *J. Geophys. Res.*, *92*, 3027–3049, 1987.

J. R. Campbell, Science Systems and Applications, Inc., Greenbelt, MD 20771.

S. A. Christopher, Department of Atmospheric Sciences, University of Alabama in Huntsville, Huntsville, AL 35805, USA.

P. R. Colarco, University of Colorado, LASP/PAOS, Boulder, CO 80309, USA.

D. P. Eleuterio and H. H. Jonsson, Naval Postgraduate School, Monterey, CA 93943, USA.

B. N. Holben, L. A. Remer, and S.-C. Tsay, NASA Goddard Space Flight Center, Greenbelt, MD 20771, USA.

J. M. Livingston, SRI International, Menlo Park, CA 94025, USA.

J. E. Kinney, Space and Naval Warfare Systems Center-San Diego, 53560 Hull Street, San Diego 92152,CA, USA.

H. B. Maring, J. M. Prospero, and D. L. Savoie, Rosenstiel School of Marine and Atmospheric Science, University of Miami, Miami, FL 33149, USA.

M. L. Meier, Material Science and Chemical Engineering, University of California, Davis, CA 95616, USA.

P. Pilewskie and P. B. Russell, NASA Ames Research Center, Mountain View, CA 94035, USA.

E. A. Reid, J. S. Reid, and D. L. Westphal, Naval Research Laboratory, 7 Grace Hopper Street, Stop 2, Monterey, CA 93943-5502, USA. (reidj@nrlmry.navy.mil)

A. Smirnov, University of Maryland Baltimore County, Baltimore, MD 21250, USA.

D. Tanré, Laboratoire d'Optique Atmospherique, CNRS, Universite des Sciences et Technologies de Lille, 59655, Villeneuve d'Ascq cedex, France.

E. J. Welton, Laboratory for Atmospheres, NASA GSFC Code 912, Building 33, Room A415, Greenbelt, MD 20771, USA.